7-17-1966

Nucleate boiling heat transfer from a rotating horizontal cylinder to saturated water.

J. Todd McLean
University of Windsor

NUCLEATE BOILING HEAT TRANSFER

FROM A ROTATING HORIZONTAL CYLINDER

TO SATURATED WATER

A Thesis

Submitted to the Faculty of Graduate Studies through the Department of Mechanical Engineering in Partial Fulfillment of the Requirements for the Degree of Master of Applied Science at the University of Windsor

By

J. Todd McLean

B.A.Sc., University of Windsor, 1965

Windsor, Ontario, Canada

1966

UMI Number: EC52617

ProQuest Information and Learning Company
789 East Eisenhower Parkway
P.O. Box 1346
Ann Arbor, MI 48106-1346

ABF 7549

APPROVED BY:

A. A. Lisot

N. G. Colborne

C. St. Pierre

101990

ABSTRACT

The influence of rotation on boiling heat transfer coefficients has been investigated. A cylindrical horizontal heating element was rotated about its axis at speeds of 0 - 800 RPM and a maximum increase in the rate of heat transfer of approximately 100% was found to occur when the rotational Reynolds number was equal to 14,500. For rotational Reynolds numbers greater than this value, the rate of heat transfer was decreased to values less than those occurring at very low speeds of rotation.

The data was well correlated by the expression :

$$Q = 625 \cdot k \cdot (Pr)^{1/3} (\Delta T)^{1.82} (M)^{-0.39}$$

for $1 < M < 8$

ACKNOWLEDGEMENTS

The author wishes to express his gratitude to the following: Dr. A.A. Nicol for his supervision and encouragement; Mr. R. Myers and Mr. O. Brudy of the machine shop for their help; and the National Research Council for their financial assistance.

TABLE OF CONTENTS

LIST OF FIGURES

NOMENCLATURE

The following symbols were used in this paper:

a	acceleration, ft/hr^2
A	effective heater surface area, ft^2
B	constant defined by equation (2.9)
C	constant pressure heat capacity, Btu/lb-°F
C_1	constant defined by equation (2.2)
C_2	constant defined by equation (2.7)
C_3	constant defined by equation (5.1)
C_4	constant defined by equation (5.3)
C_5	constant defined by equation (5.6)
C_{sf}	constant defined by equation (2.14)
D	heater diameter, ft
f, f_1, f_2	functions
g	acceleration due to gravity, ft/hr^2
g_1	function
g_o	conversion factor
G	a/g
G_v	vapour mass velocity, $lb/hr\text{-}ft^2$
h	heat transfer coefficient, $Btu/hr\text{-}ft^2\text{-}°F$
h_{fg}	latent heat of vaporization, Btu/lb
k	thermal conductivity, Btu/hr-ft-°F

m	constant defined by equation (2.2)
M	variable defined by equation (5.2)
n	number of active bubble sites
P	absolute pressure, lb/ft^2
q	heat transfer rate, Btu/hr
Q	heat flux, $Btu/hr\text{-}ft^2$
T	temperature, °F
ΔT	$= \Delta T_{sat} = T_w - T_s$, °F
y	constant defined by equation (5.3)
z	constant defined by equation (5.7)
Gr	Grashof number
Nu	Nusselt number
Pr	Prandtl number
Re_b	bubble Reynolds number
Re_R	rotational Reynolds number
Re_v	vapour Reynolds number
St	Stanton number
α	thermal diffusivity, ft^2/hr
β	coefficient of thermal expansion, 1/°R
Φ	constant defined by equation (2.10)
ρ	density, lb/ft^3
σ	surface tension, lb/ft
μ	dynamic viscosity, lb/ft-hr
ω	angular velocity, 1/hr

Subscripts

b	bubble
crit	critical
l	liquid
R	rotational
s	saturated liquid
v	saturated vapour
w	wall

CHAPTER I

INTRODUCTION

With the development of high heat production devices such as the jet engine, rocket nozzle, and nuclear reactor, where heat transfer rates are of the order of 10^6 to 10^7 Btu/hr-ft^2, considerable interest has developed in the boiling process. With its high heat transfer rates at modest temperature differences, the boiling process offers one good method of removing these large quantities of heat.

The purpose of this research is to investigate the effect of rotation of a horizontal cylindrical heating element about its axis on the rate of heat transfer from the heating surface to saturated water in the nucleate boiling regime.

The rotating element was electrically heated and measurements were taken over a range of rotational Reynolds numbers from 3,000 to 83,000, with a maximum heat flux of 25,000 Btu/hr-ft^2.

CHAPTER II

LITERATURE SURVEY

Pool boiling data is separable into six principal regimes. Of primary interest in this investigation are the three regimes I, II, and III, as given by Hsu [1], (fig. 1). Heat transfer in the first regime occurs by the mechanism of free convection as the heating element surface temperature T_w is raised above the saturation temperature of the liquid. With a further increase in T_w, nucleate boiling begins and vapour bubbles form at favoured positions, or "nucleation sites" on the heated surface (regime II). These bubbles detach from the surface but condense before reaching the surface of the pool. Further increases in T_w result in an increase in the number of vapour bubbles forming on the heated surface which do not condense but increase in size before reaching the pool surface (regime III). Beyond the peak of the curve is the transition boiling regime IV, where an unstable vapour film forms around the surface and collapses and reforms rapidly. This film provides additional resistance to the transfer of heat, thus reducing the heat transfer rate.

In regime V, the film ceases to collapse and reform repeatedly but the shape of the film varies continuously.

In regime VI, the influence of radiation becomes pronounced and the film is very stable.

2.1 MECHANISM OF NUCLEATE BOILING HEAT TRANSFER

The model for nucleate boiling suggested by Hsu and Graham [2] is as follows (fig. 2): a uniformly heated surface is considered with a liquid above it. This surface is imperfect with small cavities distributed over it, each of these cavities being a potential site for a bubble nucleus. A vapour bubble will develop at one of these sites provided that a proper superheated thermal layer is established above the site. This stage is termed "the development of the thermal layer."

The next stage of bubble growth occurs when the bubble nucleus begins a rapid growth period. This stage was investigated by Hsu and Graham using a Schlieren technique and it was observed that the growing bubble displaced the thermal layer as far away from the nucleation site as one bubble diameter. This stage is termed "the bubble growth period."

When the bubble leaves the heating surface, the thermal layer in the vicinity is destroyed and cooler liquid covers the heating surface around the nucleation site. This stage is called "the destruction of the thermal layer."

The relatively cold liquid requires a definite time period to warm up to the critical superheated condition; then the nucleate boiling cycle repeats the above-mentioned stages.

To be of general use, it is necessary that the data of the many researchers be correlated in some useable form. Boiling heat transfer is however, so complex and the fluid motion so apparently random that a single equation cannot correlate the data over the entire range of ΔT represented in figure 1. Hence separate correlations are required for each regime.

In addition to the basic variables considered for purely convective heat transfer processes, ie: density, thermal conductivity, and specific heat, some of the other variables to be considered are: surface tension, latent heat of vaporization, saturation temperature, density of the vapour, plus other properties of both liquid and vapour. Also to be considered are geometry, mass flow, and the character of the heating surface such as the type of metal, roughness, and adsorbed gas.

2.2 CORRELATION OF HEAT TRANSFER DATA IN REGIME I

McAdams [3] has taken most of the available experimental data for heat transfer by natural convection from stationary horizontal cylinders ranging in diameter from 0.002 inches to 1 foot and has found that this data is well correlated by an expression of the form:

$$Nu = f(Gr \cdot Pr) \tag{2.1}$$

For $Gr \cdot Pr > 10^4$, the correlation is of the form:

$$Nu = C_1 \cdot (Gr \cdot Pr)^m \tag{2.2}$$

King [4] has determined the constants C_1 and m as:

$$C_1 = 0.525, \ m = 1/4 \ ; \quad 10^4 < Gr \cdot Pr < 10^9 \tag{2.2.1}$$

$$C_1 = 0.129, \ m = 1/3 \ ; \quad Gr \cdot Pr > 10^9 \tag{2.2.2}$$

where all the fluid properties are evaluated at the mean film temperature with the exception of β which is evaluated at the bulk fluid temperature.

For the case where the horizontal cylinder is rotated about its axis, Becker [5] , using dimensional analysis, suggested that the convective heat transfer data could be correlated by an equation of the form:

$$Nu = g(Re_R, Gr, Pr) \qquad (2.3)$$

where $$Re_R = \frac{\omega D^2 \rho}{2\mu} \qquad (2.3.1)$$

Anderson and Saunders [6] found however that for a cylinder rotating horizontally in air below a critical value of Reynolds number, the Nusselt number was independent of the rotational Reynolds number and the rate of heat transfer was mainly determined by free convection. Above this critical value, the Nusselt number increased with Reynolds number and the effect of the Grashof number was negligible. These findings were also observed by Dropkin and Carmi [7]. Anderson and Saunders also suggested that above the critical value of rotational Reynolds number the flow patterns set up by the rotating cylinder were in many respects analagous to the irregular flow which occurs in free convection above a heated horizontal plate. They solved the problem for air and Becker applied the analogy to the general case of any fluid. His result was:

$$Nu = 0.111\ Re_R^{2/3} . Pr^{1/3} \qquad (2.4)$$

which compared very well with his empirical correlation:

$$Nu = 0.133\ Re_R^{2/3} . Pr^{1/3} \qquad (2.5)$$

Merte and Clark [8] and Graham and Hendricks [9] investigated the influence on boiling of a force field directed normal to the heating element. These investigations were carried out with the heater tank mounted on the end of a centrifuge arm. Merte and Clark found that the heat transfer data in the free convection regime for accelerations from 1 to 21 G's could be correlated by the expression:

$$Nu = 0.0505 \cdot (Gr \cdot Pr)^{0.396} \tag{2.6}$$

with g in the Grashof number replaced by the acceleration.

The results of Graham and Hendricks indicate in general that increased acceleration does indeed improve natural convection. They found that the increase in the rate of heat transfer was proportional to the Grashof number raised to the 0.25 power, ie:

$$Nu = C_2 \cdot (Gr)^{0.25} \tag{2.7}$$

Graham and Hendricks do not give sufficient information on the construction of their equipment to properly explain the discrepancy between equations (2.6) and (2.7); however it was noted that Merte and Clark employed flow guides in the heater tank which effectively increased the exponent in their correlation from 1/3 as in equation (2.2.2) to 0.396 in equation (2.6).

2.3 CORRELATION OF HEAT TRANSFER DATA IN REGIMES II & III

Merte and Clark, and Graham and Hendricks, also investigated the effect of centrifugally created accelerations on nucleate pool boiling. Merte and Clark did not attempt a correlation of the data because (a) the quantity of the data was small, and (b) the data was for one Prandtl number only. Graham and Hendricks were primarily concerned with observing the effect of acceleration so they too did not attempt a correlation. However the general results obtained by the authors which are of interest to this investigation on a comparison basis are as follows:

(1) Acceleration at low heat flux considerably increases the heat transfer rate for a given temperature difference; at high heat flux, acceleration has little effect on the boiling mechanism. It is noted though that for an acceleration of 21 G's, the heat flux is slightly less than the flux at 1 G for the same temperature difference.

(2) A small amount of subcooling has a pronounced effect on the boiling curve and it appears that subcooling is a more significant parameter than

acceleration in determining the heat transfer associated with boiling.

(3) Near the incipient boiling condition, an increase in acceleration decreases the number of active sites.

(4) The heater tank geometry does influence the rate of heat transfer.

Costello, Adams, and Clinton [10] studied the effect of centifugally-created accelerations on burnout heat flux and found that not only did increased acceleration cause an increase in the heat transfer rate but also that it increased the burnout heat flux by as much as 180%. This effect occurred because of the high buoyancy forces exerted on the vapour bubbles which tended to move them rapidly away from the heating surface in the direction of the acceleration vector.

Tien [11] employed a hydrodynamic model for nucleate pool boiling similar to that suggested by Hsu and Graham and suggested a dimensionless correlation as a function of the number of active bubble sites on the heater surface, ie:

$$q/A = 61.3 \cdot k \cdot (Pr)^{1/3}\, n^{\frac{1}{2}}\, \Delta T \qquad (2.8)$$

The work of Lienhard [12] offered some rationalized empirical corrections to the assumptions underlying equation (2.8). The corrected correlation is:

$$q/A = B \cdot k \cdot (Pr)^{1/3} \frac{\sqrt{\sigma\, g(\rho_l - \rho_v)/\rho_l^2}_{\text{INTEREST}}}{\sqrt{\sigma\, g(\rho_l - \rho_v)/\rho_l^2}_{\text{WATER}}} (\Delta T)^{5/4}\, n^{1/3} \tag{2.9}$$

where B is a constant to be determined by experiment and water is the reference fluid.

A bold approach to the correlation of nucleate boiling heat transfer data was made by Gilmour [13]. He proposed that an equality be written of three familiar dimensionless groups together with a new dimensionless group to take care of pressure and surface tension. The expression is:

$$\left(\frac{h}{C \cdot G_v}\right)^a \left(\frac{C\,\mu}{k}\right)^b \left(\frac{\rho_l \sigma}{P^2}\right) = \frac{\Phi}{(DG_v/\mu)^d} \tag{2.10}$$

The vapour mass velocity is defined as:

$$G_v = \frac{V \cdot \rho_l}{V \cdot \rho_v} = \frac{(q/A)\rho_l}{h_{fg}\, \rho_v} \tag{2.11}$$

where V is the mass of vapour produced per unit time.

Since the exponent of the Stanton number is usually unity, it was considered as such for the final correlation. In the same manner, the exponent of the Prandtl number was considered to be equal to 0.6. The exponent of the vapour Reynolds number was determined experimentally with the aid of equation (2.11) to be equal to 0.3. The final form of the correlation is then:

$$(St)(Pr)^{0.6}(Re_v)^{0.3}\left(\frac{\rho_l\,\sigma}{P^2}\right)^{0.425} = \Phi \tag{2.12}$$

The experimental data available to Gilmour was well correlated by this expression.

Rohsenow [14, 15, 16] suggested that the correlation of nucleate boiling heat transfer data could be effected by an equation of the form:

$$Nu = g_1(Re_b,\ Pr) \tag{2.13}$$

where the bubble Reynolds number measures the magnitude of the agitation associated with the turbulent flow caused by the bubble motion. The correlating equation obtained from (2.13) is:

$$\frac{C_l(\Delta T)}{h_{fg}} = C_{sf}\left(\frac{q/A}{\mu h_{fg}}\sqrt{\frac{g_0\sigma}{g(\rho_l-\rho_v)}}\right)^{1/3}(Pr)^{1.7} \tag{2.14}$$

The constant C_{sf} is dependent upon the nature of the heating surface-fluid combination and was determined by Cryder and Finalborgo [17] to be equal to 0.0060 for a brass heater in water.

McNelly [18] has suggested the following correlation for nucleate boiling heat transfer data:

$$\frac{hD}{k} = 0.225\left[\frac{DQ}{h_{fg}}\right]^{0.69}\left[\frac{PD}{\sigma}\right]^{0.31}\left[\frac{\rho_l}{\rho_v} - 1\right]\left[\frac{C\mu}{k}\right]^{0.69} \qquad (2.15)$$

Forster and Zuber have correlated their results with the following expression:

$$\left[\frac{C\rho_l\sqrt{\pi\alpha_l}\,Q}{kh_{fg}\rho_v}\right]\left[\frac{2\sigma}{\Delta P}\right]^{\frac{1}{2}}\left[\frac{\rho_l}{g_o\,\Delta P}\right]^{\frac{1}{4}} = 0.0015\left[\frac{\rho_l}{\mu_l}\left(\frac{C_l\rho_l(\Delta T)\pi\alpha_l}{h_{fg}\rho_v}\right)\right]^{0.62}\left[\frac{C_l\mu}{k_l}\right]^{0.33}. \qquad (2.16)$$

The above correlations are but a few of the number which exist in the literature.

CHAPTER III

APPARATUS and INSTRUMENTATION

The test facilities are shown schematically in figure 3.

3.1 HEATER ELEMENT

The electrical heating element employed for the tests was a Chromalox 'Redhead' cartridge heater, $\frac{3}{4}$ inch in diameter with a sheath length of $10\frac{1}{2}$ inches. The element was rated at two thousand watts for 120v A.C. input. The element was encased in a 99% pure copper sheath which was in turn connected at each end to a 0.500 inch O.D. by 0.310 inch I.D. stainless steel shaft (fig. 4). The heater power leads were led through the hollow shaft to the power slip-ring assembly.

The unit was rotated by means of an A section pulley drive with a 3:1 speed reduction ratio from a 3.5 kW (4.7 hp) adjustable speed A.S.E.A. direct current motor.

3.2 HEATER POWER SUPPLY

Electrical power was supplied to the cartridge heater from the main A.C. power line and varied by means of a Variac autotransformer, model W50H, rated at

0-280 volts for 240 volts input.

3.3 WATER TANK

The tank was constructed of one-half inch 'Plexiglas'; it measured twenty inches in length by ten inches in width by fifteen inches in height, (20 x 10 x 15"). The stainless steel shaft passed through brass glands at both ends of the tank. The glands were adjustable for leakage and were packed with temperature-resistant Teflon pump packing.

3.4 THERMOCOUPLES AND RELATED SLIP-RING ASSEMBLY

Three grooves, 1/8 by 1/8 inch were milled axially along the entire length of the sheath (fig. 4) at 120 degree intervals around the circumference for the purpose of carrying the thermocouple lead wires. At selected stations along these grooves, 1/16 by 1/4 inch slots were ground at right angles to the milled grooves. The thermocouples were placed in these slots with the measuring junctions at the sheath surface. The slots and grooves were then filled with a high-temperature thermo-setting epoxy resin. Thin copper strips were placed in the grooves covering the thermocouple lead wires and the resin was then cured.

The thermocouples were copper-constantan, #30 gauge B&S, and were placed at fifteen stations on the sheath surface. The lead wires were taken to the thermocouple slip-ring assembly via the milled grooves and then through the centre of the stainless steel shaft. The copper leads were connected to one common slip-ring. The equivalent thermocouple circuit is shown in figure 5.

The slip-ring assembly was constructed of sixteen 7/8 inch diameter rings, 5/32 inch wide, and spaced 1/8 inch apart. Phosphor bronze "brushes", with provision for adjusting brush pressure, tapped the thermocouple signal from the slip-rings. The signal was displayed by a model 2745 Honeywell potentiometer.

3.5 PREHEATERS

Two 1000 watt water heaters were mounted through the sides of the tank perpendicular to the axis of rotation of the test section, to preheat the water to boiling conditions and to ensure that the bulk water temperature did not fall below the saturation temperature.

CHAPTER IV

EXPERIMENTAL PROCEDURE

4.1 THERMOCOUPLE CALIBRATION

With no power input to the test section, the distilled water was preheated to boiling temperature. When steady state conditions were attained, measurements were taken of the water temperature by means of a mercury thermometer, six thermocouples connected in parallel and placed in the water in a circular pattern around the test section, and the thermocouples on the test section surface. This procedure was carried out before all test runs; the thermocouple measurements were always in agreement within 0.010 mV ($\pm\frac{1}{2}$°F).

4.2 THERMOCOUPLE SLIP-RING ERROR

It was observed that when the test section was rotated at any appreciable speed, a random error was introduced in the thermocouple signal due to the friction between slip-rings and brushes. This error was eliminated by periodically lubricating the slip-rings with distilled water.

4.3 TEST PROCEDURE

Each run was performed at one rotational speed. For each value of power input to the test section, beginning at 200 watts and increasing by increments of approximately 200 watts, steady state conditions were obtained and measurements of thermocouple potential made at each of the fifteen stations on the surface of the test section.

The potentials were measured individually by means of the selector switch 'E' (fig. 5). The temperature profile along the length of the test section indicated higher temperatures at the centre of the test section than existed at either end. This indicated some heat loss in the axial direction. In order for the heat transfer characteristics to be useful on a comparative basis, it was assumed that all of the heat input to the test section was dissipated radially through the walls. Hence it was assumed that the magnitude of the temperature profile was constant along the length of the test section and of a value equal to the highest recorded temperature at the middle of the test section.

For this reason, four stations were selected which best averaged to the highest measured surface temperature which was then assumed to exist at all points on the test section surface. These four thermocouples were then used for succeeding runs in conjunction with the six thermocouples immersed in the water bulk to determine the ΔT_{sat}.

The above procedure was repeated for rotational speeds of 30, 50, 106, 150, 220, 300, 325, 450, 575, 700, and 850 revolutions per minute.

The power input to the test section was measured with the wattmeter 'W' (fig. 6). The value obtained was verified periodically by means of the voltmeter 'V' and ammeter 'A.'

The surface of the test section was cleaned before each test run.

CHAPTER V

EXPERIMENTAL RESULTS

The heat flux Q was determined by assuming that the total heat input to the test section was dissipated radially through the test section surface area A.

The voltage drop in the lead wires was observed to be one volt at 100 volts applied. The error in the heat transfer coefficient was due mainly to (a) the error in ΔT_{sat} ($\simeq 3\%$) and, (b) the error in the voltage measurement (1%). Since the random error in ΔT_{sat}, given in section 4.1, was three times the magnitude of the voltage error, the voltage error was neglected in the calculations.

5.1 RESULTS AND DISCUSSION

Figures 7 to 9 show the relationship of the heat flux to the temperature difference between the test section surface and the bulk water temperature. As the speed of rotation is increased, the boiling curves are shifted to the left indicating that a smaller temperature difference is required to support the same heat flux. As the speed of rotation is increased beyond 150 RPM (Re_R = 14,500), the temperature difference required to support a given heat flux begins to increase until at relatively high speeds, the heat transfer is less, for a given ΔT, than at very low speeds. At speeds greater than 500 RPM, any increase in speed has little or no effect on the boiling curve.

This occurrence is basically the same as that observed by Merte and Clark, although the physical systems are not alike in that the fluid in this investigation is moving over the heated surface.

Figures 10 and 11 display the information from figures 7 to 9 in a different manner. From these it is apparent that at the critical speed of rotation, an increase in the rate of heat transfer of approximately 100% is obtained for a temperature difference of 8 - 10 °F.

Films of the boiling process show that for speeds less than 100 RPM, the active bubble sites are unevenly distributed over the surface of the test section, with many sites being located at the seams of the copper strips covering the thermocouple lead wires. As the speed of rotation increases, it is seen that the number of active bubble sites increases. Hence the shift to the left of the boiling curve (fig. 7) in this range of speed occurs because (a) the agitation of the water is increased due to the rotation, (b) the vapour bubbles are being forced to detach more quickly than would occur if the test section were not rotating, and (c) there exist more active bubble sites as the speed of rotation increases.

Further increases in rotational speed cause the vapour bubbles to spread evenly in a relatively thick layer around the cylinder resulting in a situation not unlike film boiling. As this blanket of bubbles spreads over the test section surface, it provides increased resistance to the transfer of heat with the resultant shift of the boiling curve to the right (fig. 9).

At speeds above 300 RPM, there is no visible change in the bubble layer and this corresponds to the results shown in figures 9 and 13, that high rotational speeds have little or no effect on the rate of heat transfer.

5.2 CORRELATION OF DATA

A correlation of the data could be attempted using any of the forms given in chapter II. It was indicated in the literature that the following correlations gave very good results for static boiling.

It was decided then that these two correlations would be modified for use in this investigation - one employing the form given by Lienhard, equation (2.9), and the other using the form given by Gilmour, equation (2.12).

5.2.1 CORRELATION ONE

The boiling correlation due to Lienhard, eq'n (2.9) is:

$$Q = B\cdot k\cdot(Pr)^{1/3}\,\frac{\sqrt{\sigma g(\rho_l-\rho_v)/\rho_l^2}_{\,INTEREST}}{\sqrt{\sigma g(\rho_l-\rho_v)/\rho_l^2}_{\,WATER}}\,(\Delta T)^{5/4}\,n^{1/3}$$

It was pointed out in chapter II, section 2.3, that Merte and Clark observed an effect of acceleration on the number of active bubble sites. This effect was also observed in this investigation. Hence if $n^{1/3}$ in equation (2.9) is replaced by $n^{1/3} = f_1(Re_R)$, and since the fluid of interest is water, then the correlation form from equation (2.9) becomes:

$$Q = C_3\cdot k\cdot(Pr)^{1/3}f_1(Re_R)(\Delta T)^{1.25} \qquad (5.1)$$

The graph of $\log\left[\frac{Q}{k(Pr)^{1/3}}\right]$ versus $\log(\Delta T)$ is shown in figure 12. The experimental points lie along the mean slope line shown. The slope of this line is 1.82 which is greater than the value 1.25 indicated by equation (5.1). This discrepancy can be explained by the fact that the test section was not polished smooth after being turned to the final diameter and it appears likely that the roughness was greater than the roughness of the test sections which were used to obtain equation (5.1). The increased roughness then provides more sites for bubble formation than would exist on a relatively smooth section and hence the heat transfer rate is increased for given values of ΔT.

Hence for any one value of Re_R:

$$\frac{Q}{k(Pr)^{1/3}} \propto (\Delta T)^{1.82} \tag{5.1.1}$$

Figure 13 shows the relationship between the constant of proportionality in equation (5.1.1) and Re_R. The curve is seen to be approximately symmetrical about the critical rotational Reynolds number. This fact makes it possible for the correlation to apply over the entire range of Re_R shown in figure 13. Defining

$$\begin{aligned} M &= Re_R/Re_{R_{crit}} \; ; \quad Re_R > Re_{R_{crit}} \\ \text{or } M &= Re_{R_{crit}}/Re_R \; ; \quad Re_R < Re_{R_{crit}} \end{aligned} \tag{5.2}$$

where $Re_{R_{crit}} = 14{,}500$ from figure 13, then the form of the correlation becomes:

$$Q = k\cdot(Pr)^{1/3}(\Delta T)^{1.82}C_4(M)^y \qquad (5.3)$$

Equation (5.3) is plotted in figure 14. The constants C_4 and y are determined as:

$$C_4 = 625$$
$$y = -0.39$$

Hence the final correlation is:

$$Q = 625\cdot k\cdot(Pr)^{1/3}(\Delta T)^{1.82}(M)^{-0.39}$$
$$\text{for } 1 < M < 8 \qquad (5.4)$$

5.2.2 CORRELATION TWO

Gilmours correlation as given in chapter II was:

$$(St)(Pr)^{0.6}(Re_v)^{0.3}\left(\frac{\rho_l \sigma}{P^2}\right)^{0.425} = \phi \qquad (2.12)$$

Equation (2.12) is modified for use in this investigation by introducing a rotational Reynolds number factor and noting that for all practical purposes, the Prandtl number and $(\frac{\rho_l \sigma}{P^2})$ remain constant.

As stated in section (2.3) the correlation was developed simply by writing an equality of four dimensionless groups in which all the main parameters involved in boiling heat transfer were incorporated. Following this procedure, a rotational Reynolds number factor, $f_2(Re_R)$, is introduced as the fifth group, in which the constant Φ is contained. Equation (2.12) then becomes:

$$(St)(Re_v)^{0.3} = f_2(Re_R) \tag{5.5}$$

For the reasons stated in section (5.2.1), the exponent of the vapour Reynolds number is expected to be greater than the value indicated in equation (5.5). Figure 15 shows the relationship between the Stanton number and the vapour Reynolds number for the various rotational Reynolds numbers. The mean slope of the experimental points and hence the exponent of Re_v is determined to be equal to 0.52.

Assuming that $f_2(Re_R) = C_5(M)^z$, where M is defined in equation (5.2), then equation (5.5) becomes:

$$(St)(Re_v)^{0.52} = C_5(M)^z \tag{5.6}$$

Equation (5.6) is plotted in figure 16. The constants C_5 and z are determined as:

$$C_5 = 0.15$$
$$z = -0.19$$

The second correlation is then:

$$(St)(Re_v)^{0.52} = 0.15(M)^{-0.19}$$
$$\text{for } 1 < M < 8 \tag{5.7}$$

Statistical methods were employed which indicated that equation (5.4) was the better correlation of the two presented.

It is noted that the correlation should be used for a design calculation only if the proposed cylinder has the same diameter as the test section employed in this investigation. It is likely that a cylinder of a different diameter will also have a different critical speed of rotation. However once this new value of $Re_{R_{crit}}$ is determined, then the correlation should apply provided that the surface roughness, material, and fluid used, is the same as that used in this investigation.

5.3 DISCUSSION OF GRAPHS

Figure 13 shows how the rate of heat transfer varies with the speed of rotation. It is apparent from this curve that the heat transfer rate is less for rotational Reynolds numbers greater than 20,000 than for very low Re_R. Hence any appreciable increase in the heat transfer rate over the static case will occur for Re_R in the range 0 - 20,000. The maximum increase occurs at the critical Reynolds number value of 14,500.

It is pointed out that the experimental point scatter in figures 13, 14, and 16 is mainly normal boiling scatter which is to be expected in all boiling investigations. In figure 14 however, the scatter is also due to the fact that the curve was drawn by assuming the curve of figure 13 to be symmetrical about the critical rotational Reynolds number of 14,500. The fact that the curve of figure 13 is slightly asymmetrical leads to the increased scatter in the correlation shown in figure 14.

CHAPTER VI

CONCLUSIONS

The findings of this paper are summarized below:

a) For values of rotational Reynolds numbers below the critical value, an increase in the speed of rotation causes an increase in the heat flux for a constant heater-water temperature difference.

b) Above the critical value of rotational Reynolds number, an increase in speed decreases the heat flux for a constant ΔT.

c) For $Re_R \gg Re_{R_{crit}}$, there is little or no change in the rate of heat transfer ... there is less heat transfer at high rotational speeds than at very low speeds.

d) An increase in the heat transfer rate of approximately 100% is attained at the critical value of rotational Reynolds number.

e) At low values of Re_R less than the critical value, an increase in the speed of rotation causes an increase in the number of active bubble sites. This is the reverse effect to that found by other workers to occur near the incipient boiling condition, ie: an increase in acceleration causes a decrease in the number of active bubble sites.

f) The experimental results can be correlated by:

$$Q = 625 \cdot k \cdot (Pr)^{1/3} (\Delta T)^{1.82} (M)^{-0.39}$$

for $1 < M < 8$

BIBLIOGRAPHY

1.	Hsu, S.T.	Engineering Heat Transfer, D. Van Nostrand Co. Inc., Princeton N.J. (1963)
2.	Hsu, Y. Graham, R.W.	An Analytical and Experimental Study of the Thermal Boundary Layer and Ebullition Cycle in Nucleate Boiling, NASA Technical Note D-594 (May 1961)
3.	McAdams, W.H.	Heat Transmission, McGraw-Hill Book Co., N.Y. (1954)
4.	King, W.J.	Heat Transfer to Boiling Liquids, Refrg. Engrg., No. 25, p 83 (1933)
5.	Becker, K.M.	Measurements of Convective Heat Transfer from a Horizontal Cylinder Rotating in a Tank of Water, Int. J. Heat and Mass Transfer, Vol. 6, p 1053 (1963)
6.	Anderson, I.T. Saunders, O.A.	Convection From An Isolated Heated Horizontal Cylinder Rotating About Its Axis, Proc. Roy. Soc. A, No. 217, p 555 (1953)
7.	Dropkin, D. Carmi, A.	Natural Convection Heat Transfer from a Horizontal Cylinder Rotating in Air, ASME Trans., Vol. 79, p 741, (1957)
8.	Merte, H. Clark, J.A.	Pool Boiling in an Accelerating System, ASME Journal of Heat Transfer, p 233 (1961)
9.	Graham, R.W. Hendricks, R.C.	A Study of the Effect of Multi-G Accelerations on Nucleate Boiling Ebullition, NASA Tech. Note D-1196 (May 1963)
10.	Costello, C.P. Adams, J.M. Clinton, W.W.	Improvement of Burnout Heat Flux by Orientation of Semi-Circular Heaters, AIChE Journal, Vol. 8, No. 4, p 569 (1962)
11.	Tien, C.L.	A Hydrodynamic Model for Nucleate Pool Boiling, Int. Journal Ht. Mass Transfer, Vol. 5, p 533 (1962)

12. Lienhard, J.H. — A Semi-Rational Nucleate Boiling Heat Flux Correlation, Int. Journal Ht. Mass Transfer, Vol, 6, p 215 (1963)

13. Gilmour, C.H. — Nucleate Boiling-A Correlation, Chem. Eng. Progress, Vol 54, No. 10, p 77 (Oct. 1958)

14. Rohsenow, W.M. — A Method of Correlating Heat Transfer Data for Surface Boiling of Liquids, ASME Trans., Vol. 74, p 969 (1952)

15. Rohsenow, W.M. — Heat Transfer with Evaporation, Heat Transfer Symposium, U of M (1952)

16. Rohsenow, W.M., Choi, H.Y. — Heat, Mass, and Momentum Transfer, Prentice-Hall Inc., Englewood Cliffs, N.J. (1961)

17. Cryder, D.S., Finalborgo, A.C. — Heat Transmission from Metal Surfaces to Boiling Liquids: Effect of Temperature of the Liquid on Film Coefficient, AIChE Trans., Vol. 33, p 346 (1937)

18. McNelly, M.J. — J. Imp. Coll. Chem. Eng. Soc., Vol. 7, p 18 (1953)

19. Forster, H.K., Zuber, N. — AIChE Journal, Vol. 1, p 531 (1955)

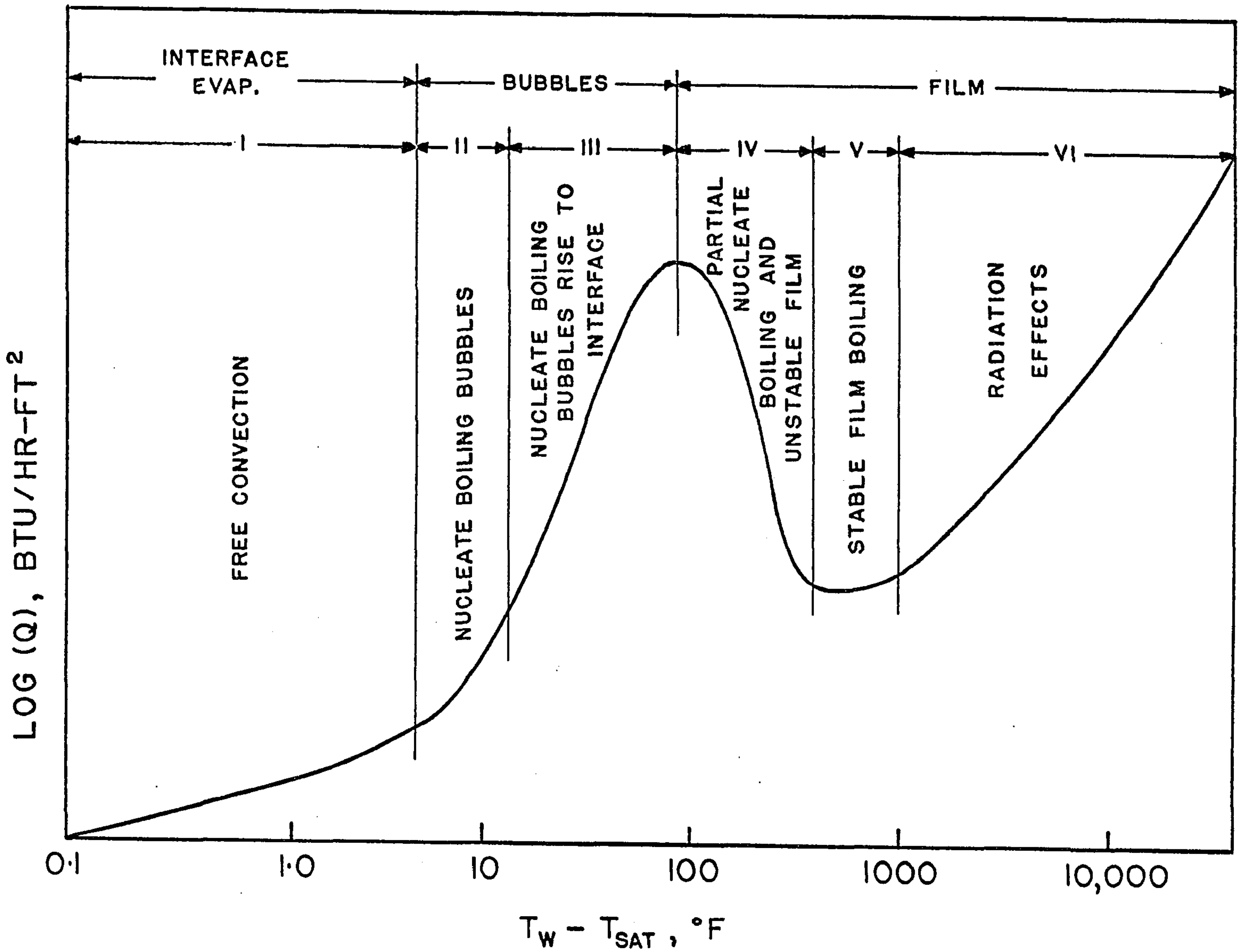

TYPICAL POOL BOILING CURVE

FIG. 1.

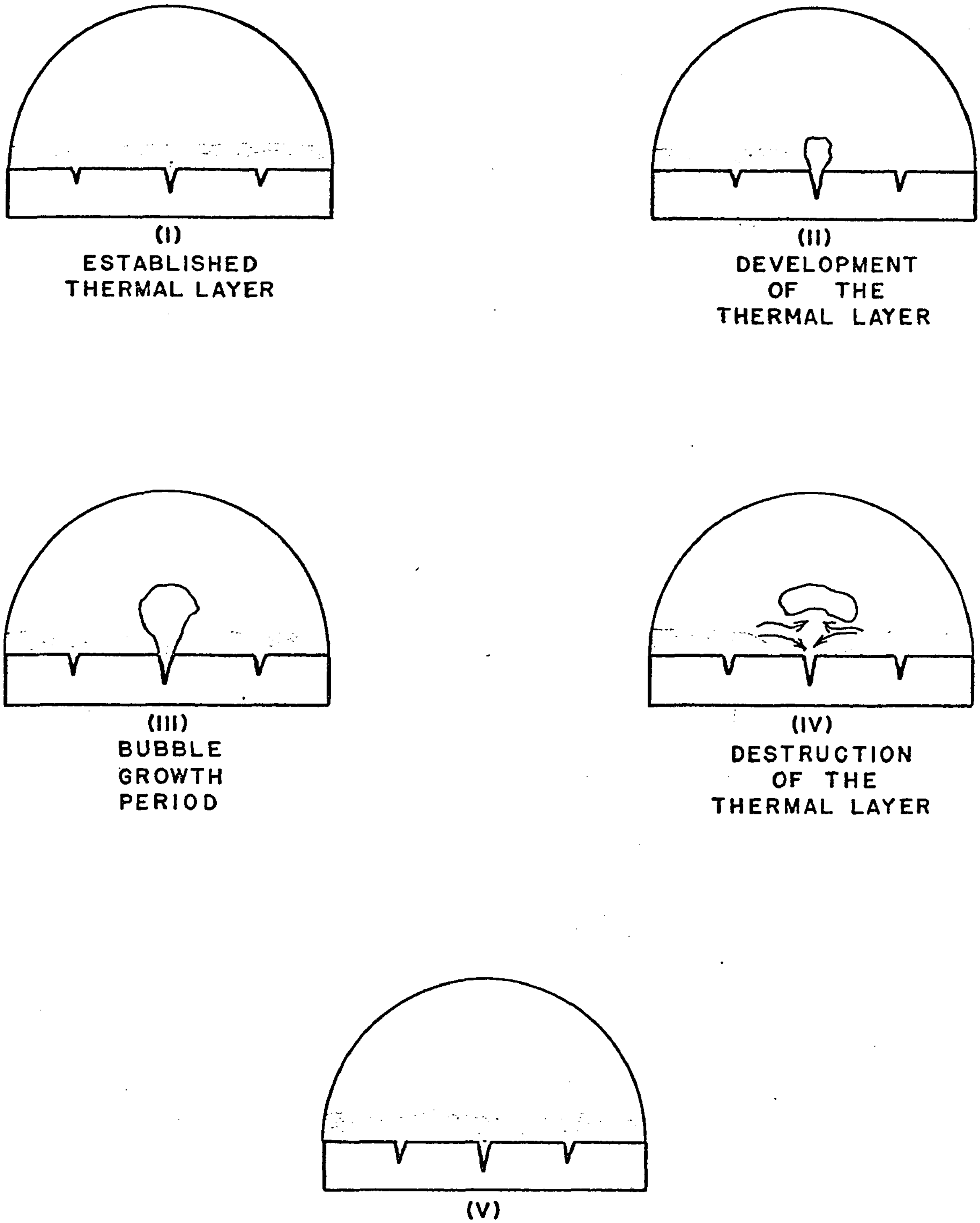

NUCLEATE BOILING MODEL

FIG. 2

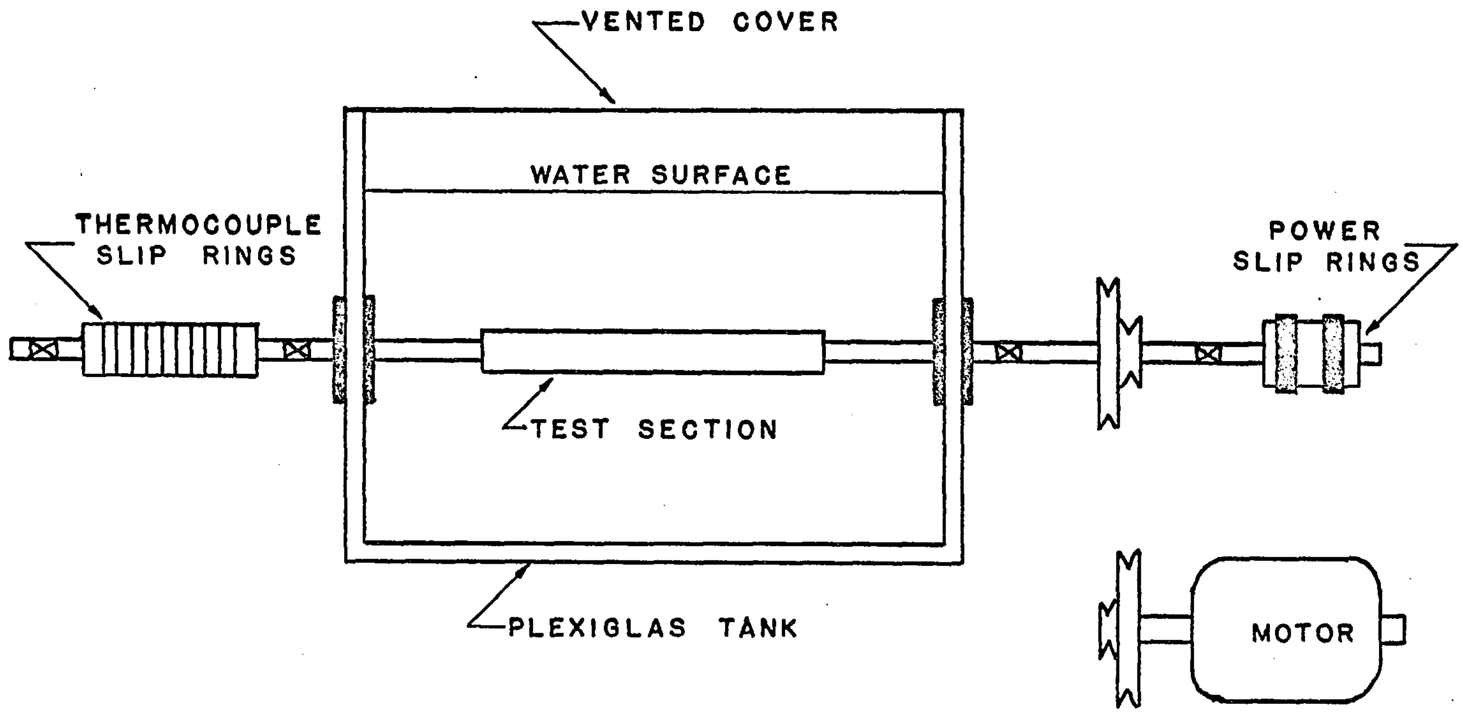

SCHEMATIC OF TEST FACILITIES

FIG. 3

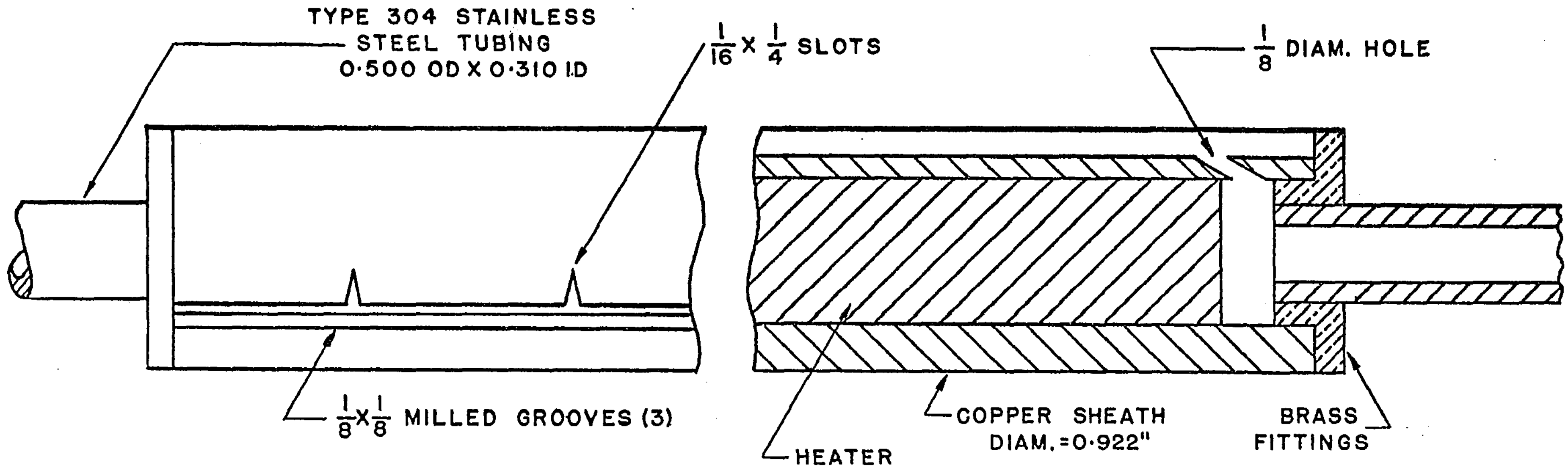

TEST SECTION

FIG. 4

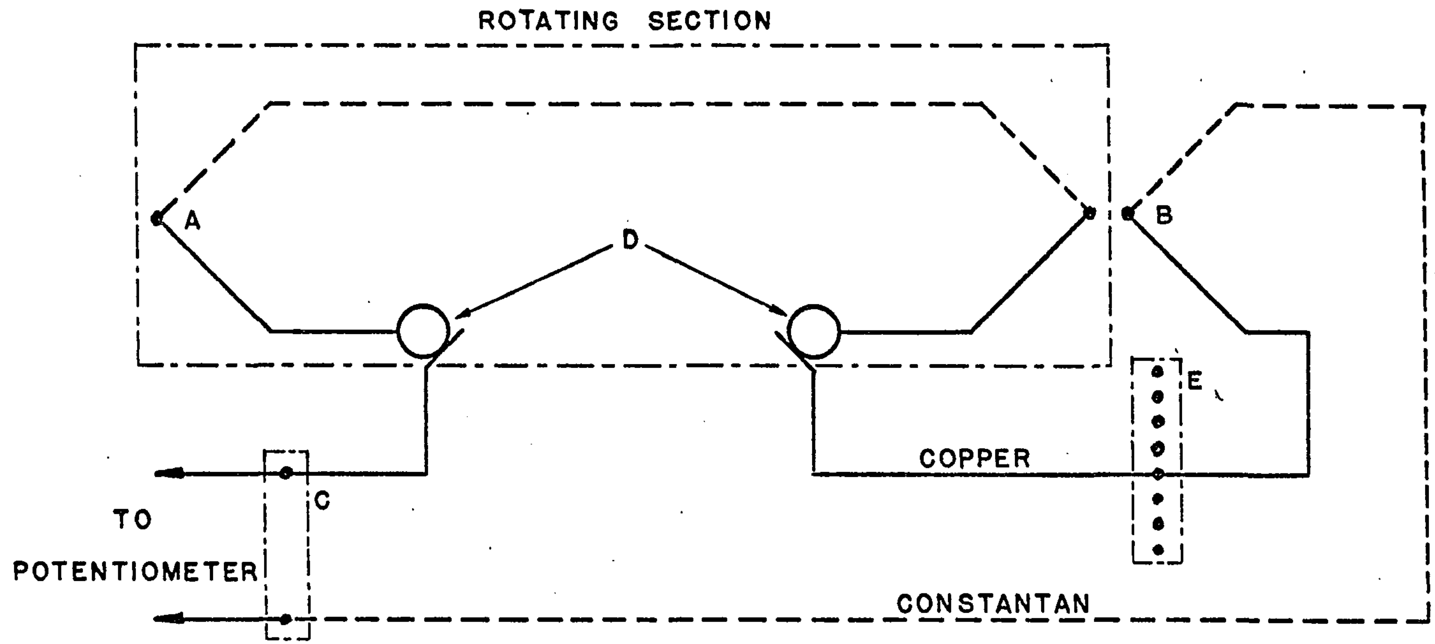

A = MEASURING JUNCTION
B = COMPENSATING JUNCTION
C = REFERENCE JUNCTION
D = SLIP RINGS & BRUSHES
E = SELECTOR SWITCH

EQUIVALENT THERMOCOUPLE CIRCUIT

FIG. 5

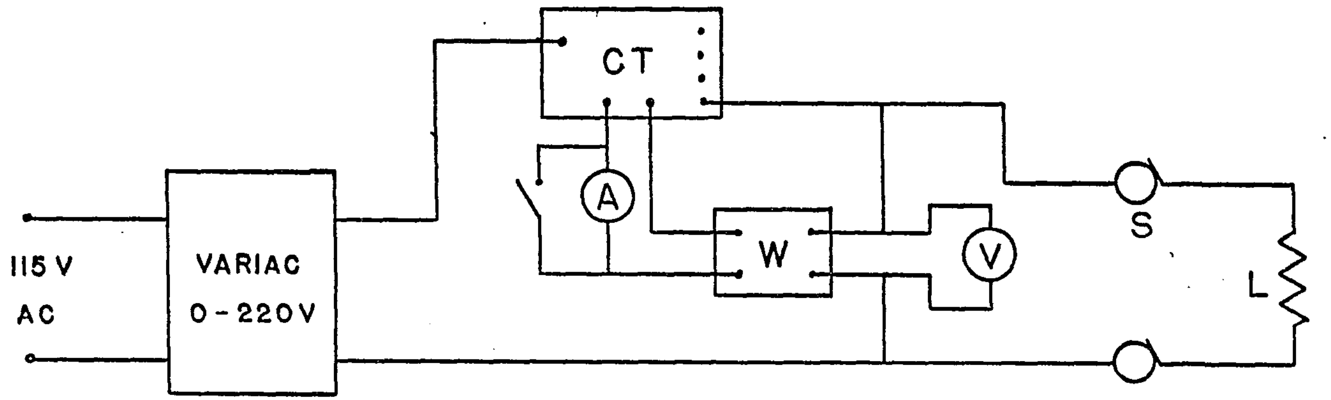

A = AMMETER
W = WATTMETER
V = VOLTMETER
CT = CURRENT TRANSFORMER
S = SLIP RINGS
L = HEATER

SCHEMATIC OF POWER CIRCUIT

FIG. 6

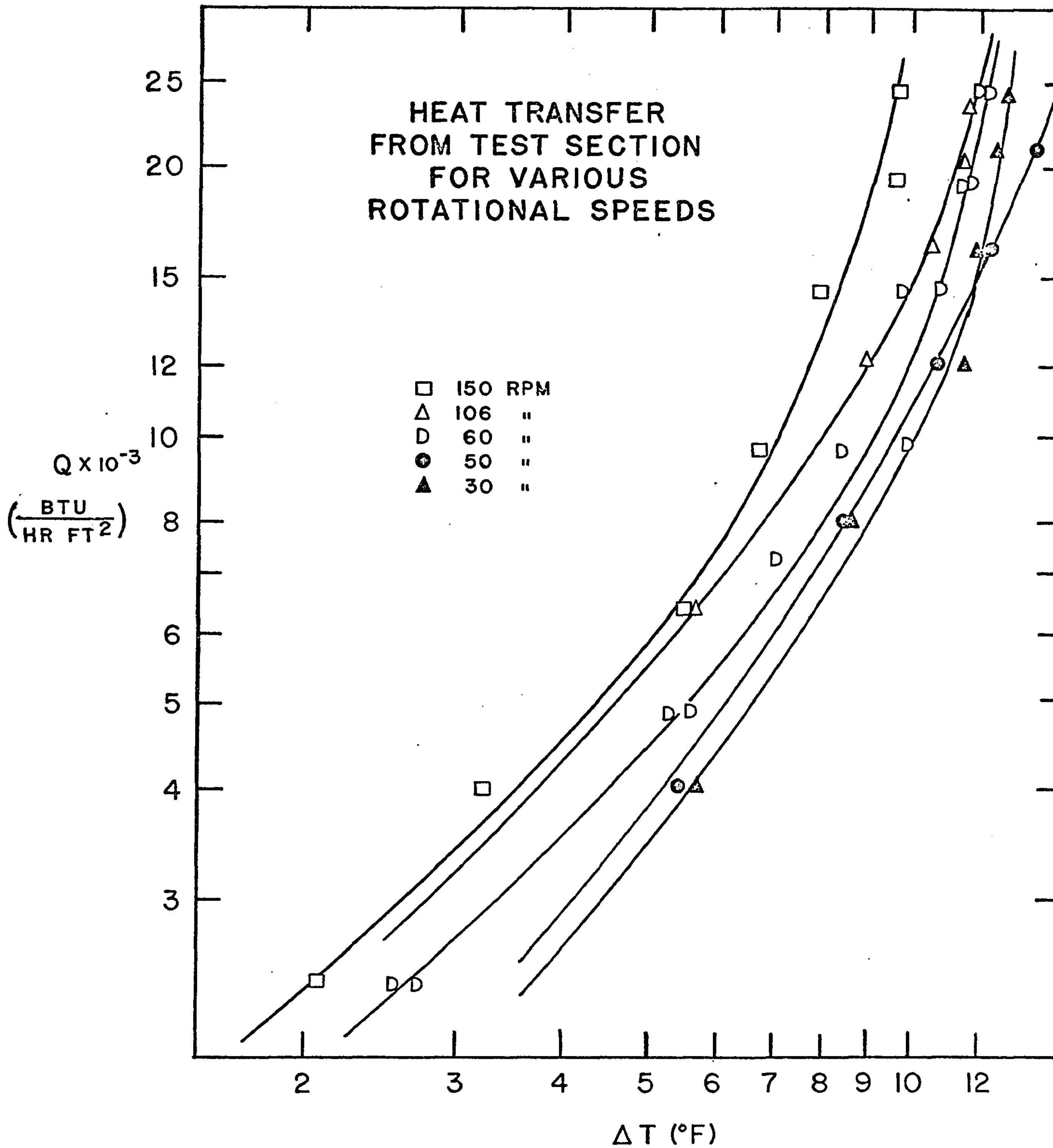
HEAT TRANSFER
FROM TEST SECTION
FOR VARIOUS
ROTATIONAL SPEEDS
150 RPM
106 "
60 "
50 "
30 "
Q x 10^-3
(BTU / HR FT²)
25
20
15
12
10
8
6
5
4
3
2
3
4
5
6
7
8
9
10
12
ΔT (°F)

FIG. 7

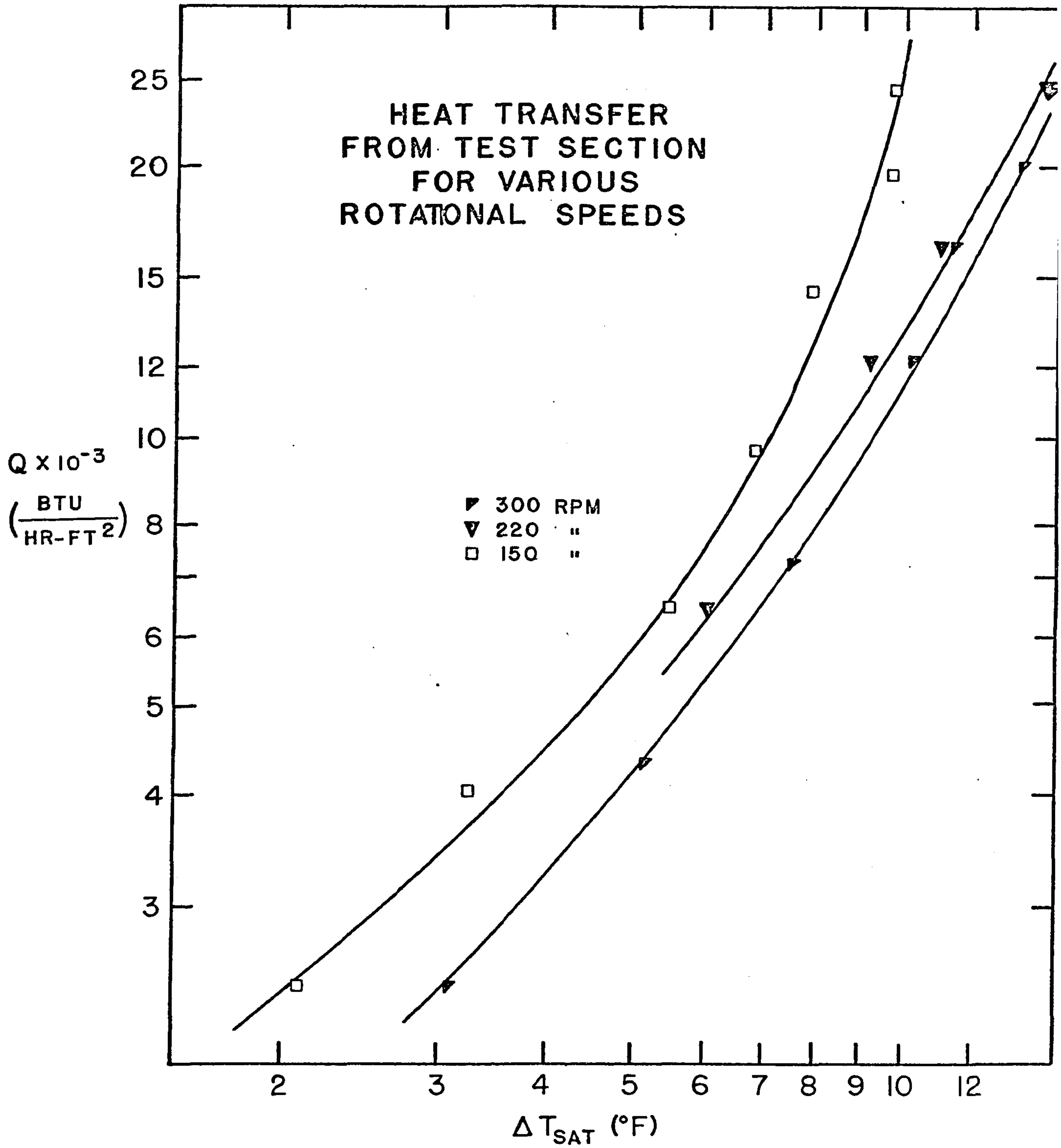
HEAT TRANSFER
FROM TEST SECTION
FOR VARIOUS
ROTATIONAL SPEEDS
300 RPM
220 "
150 "
Q x 10^-3
(BTU / HR-FT^2)
25
20
15
12
10
8
6
5
4
3
2
3
4
5
6
7
8
9
10
12
ΔT_SAT (°F)

FIG. 8

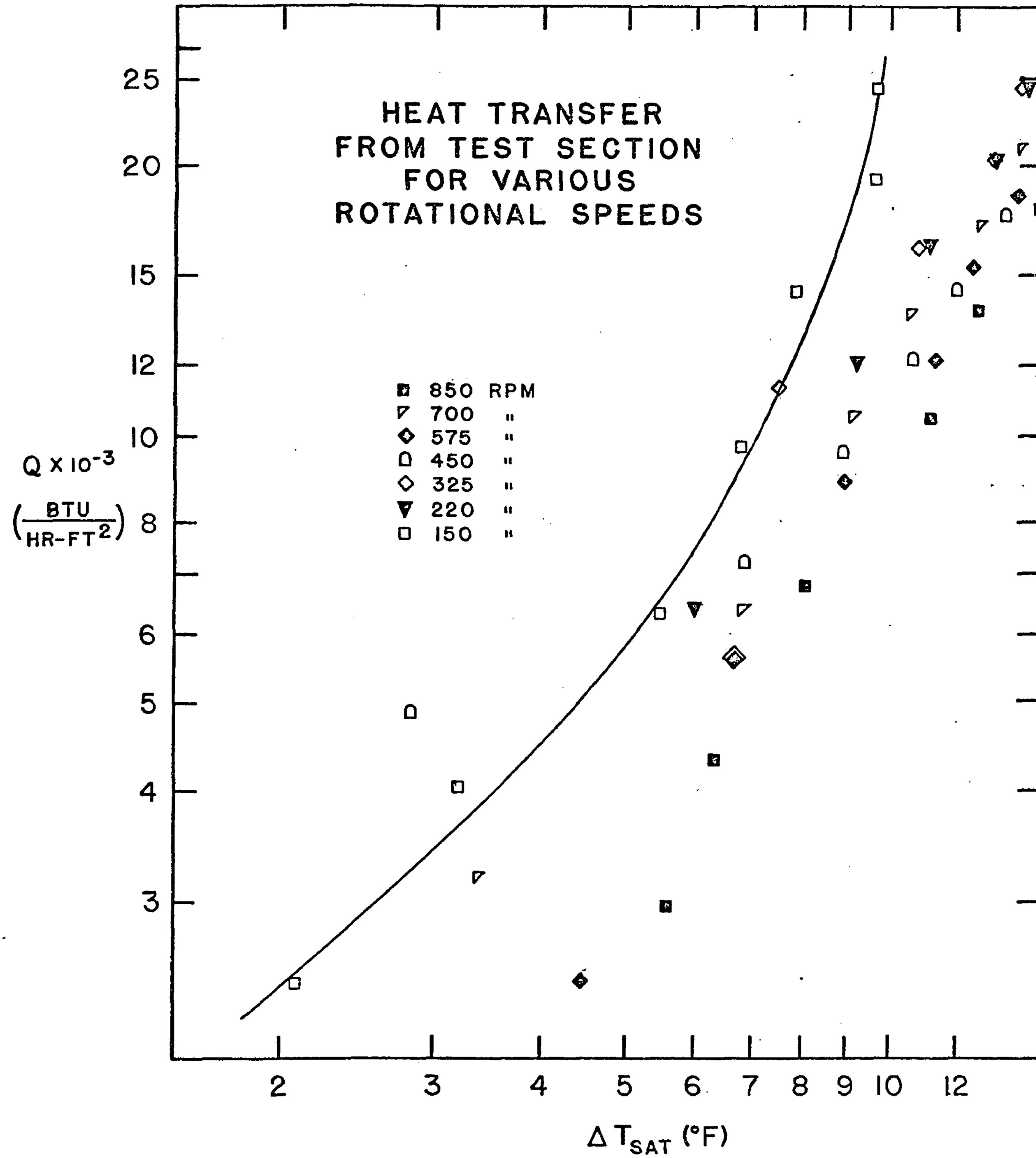
HEAT TRANSFER
FROM TEST SECTION
FOR VARIOUS
ROTATIONAL SPEEDS
850 RPM
700 "
575 "
450 "
325 "
220 "
150 "
Q x 10-3
(BTU / HR-FT2)
25
20
15
12
10
8
6
5
4
3
2
3
4
5
6
7
8
9
10
12
Δ TSAT (°F)

FIG. 9

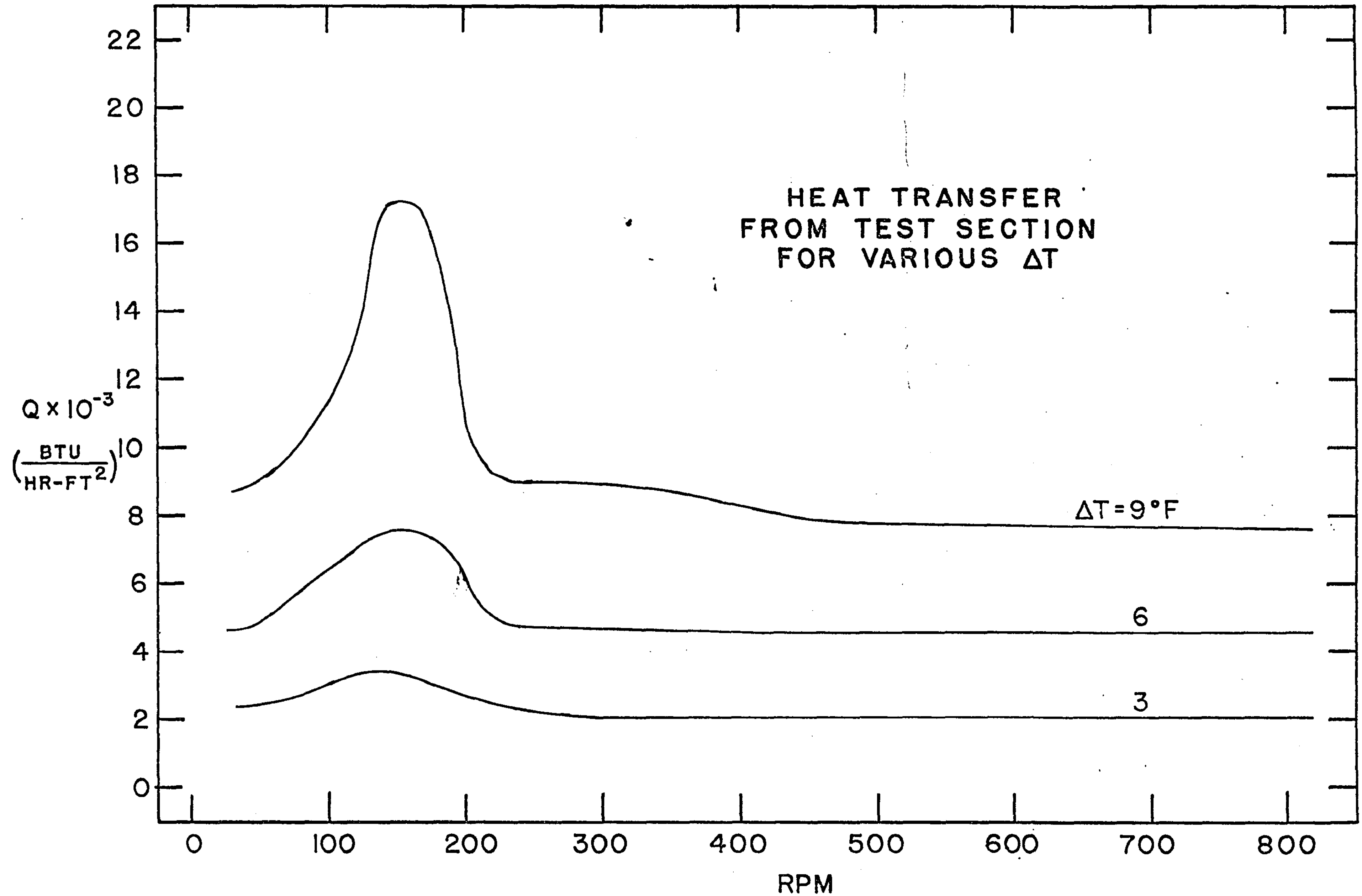
HEAT TRANSFER
FROM TEST SECTION
FOR VARIOUS ΔT
Q × 10^-3
(BTU/HR-FT^2)
22
20
18
16
14
12
10
8
6
4
2
0
ΔT=9°F
6
3
0
100
200
300
400
500
600
700
800
RPM

FIG. 10

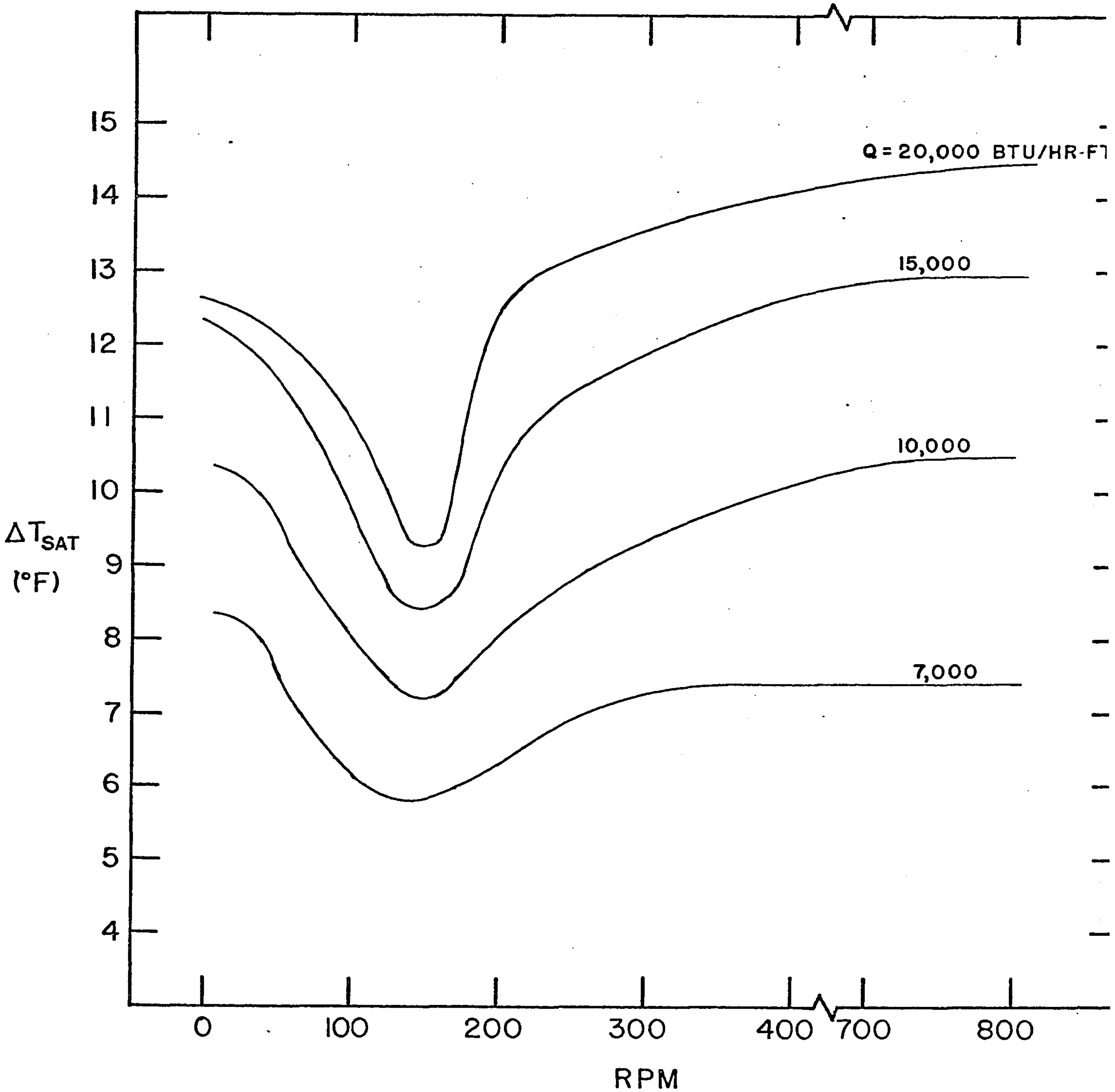

FIG. 11

EFFECT OF SPEED ON ΔT

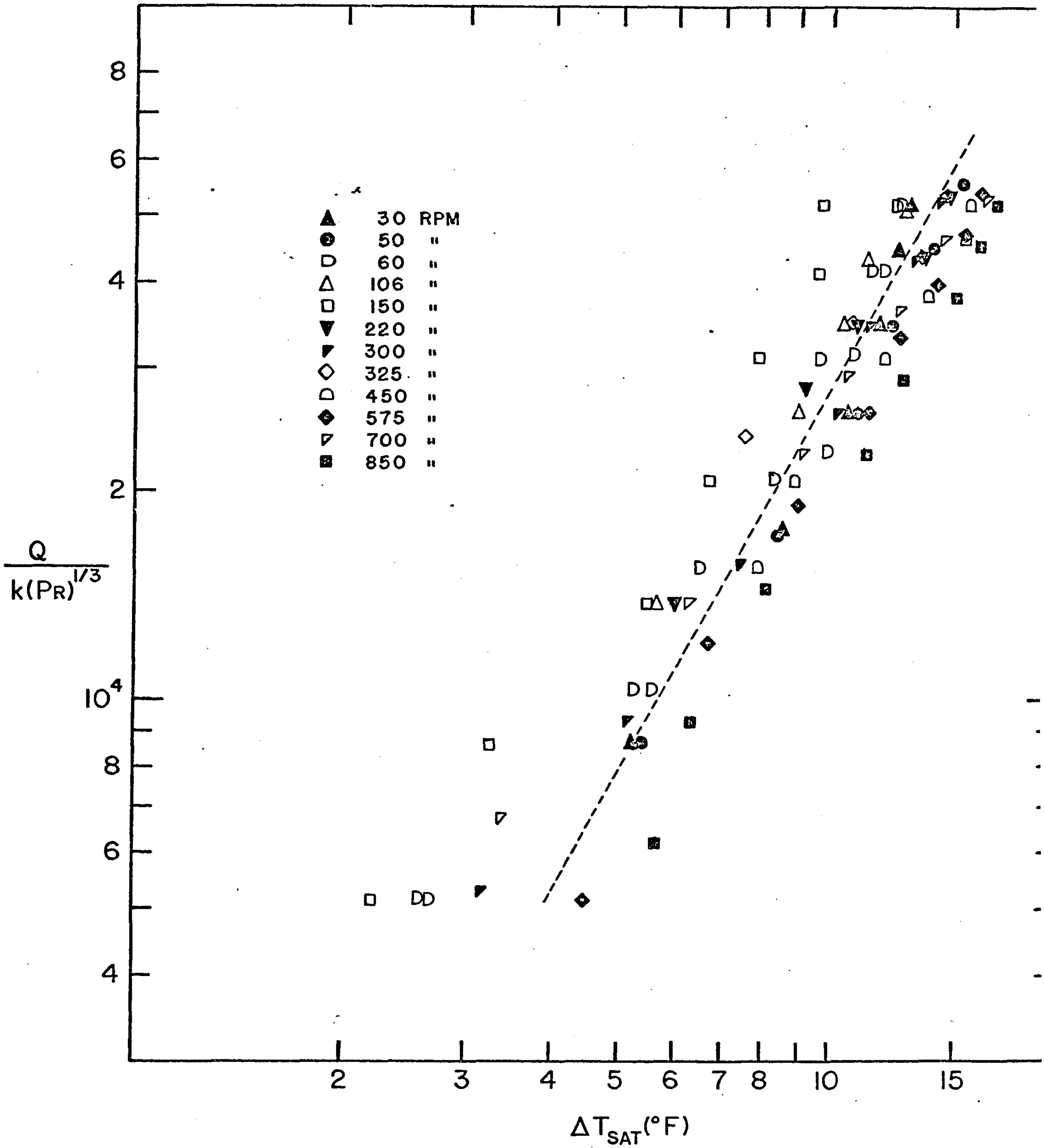

FIG. 12

CURVE TO DETERMINE THE EXPONENT
OF ΔT IN EQUATION 5.1.1

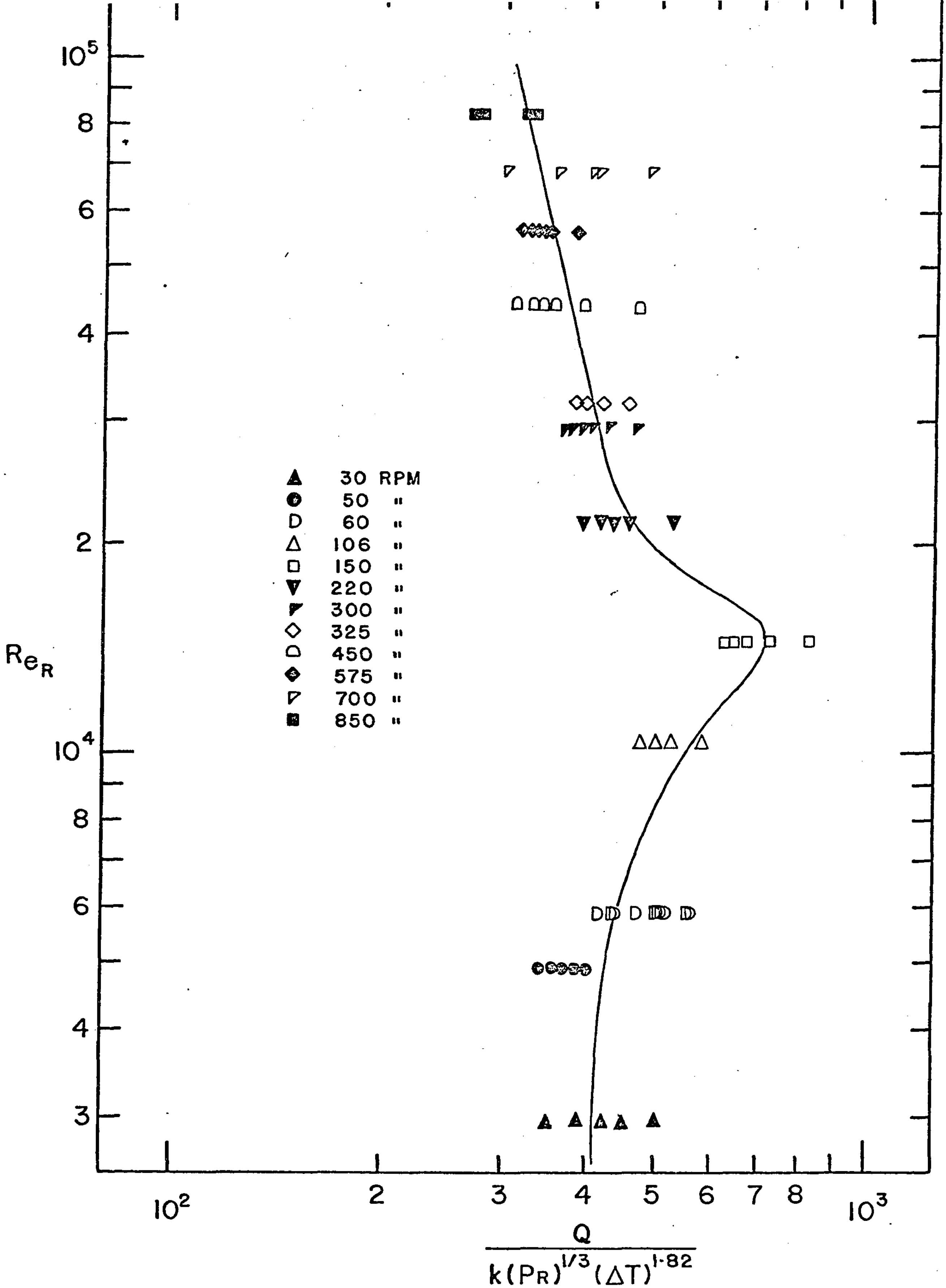

FIG. 13

RELATIONSHIP OF EQUATION 5.1.1 AND Re_R

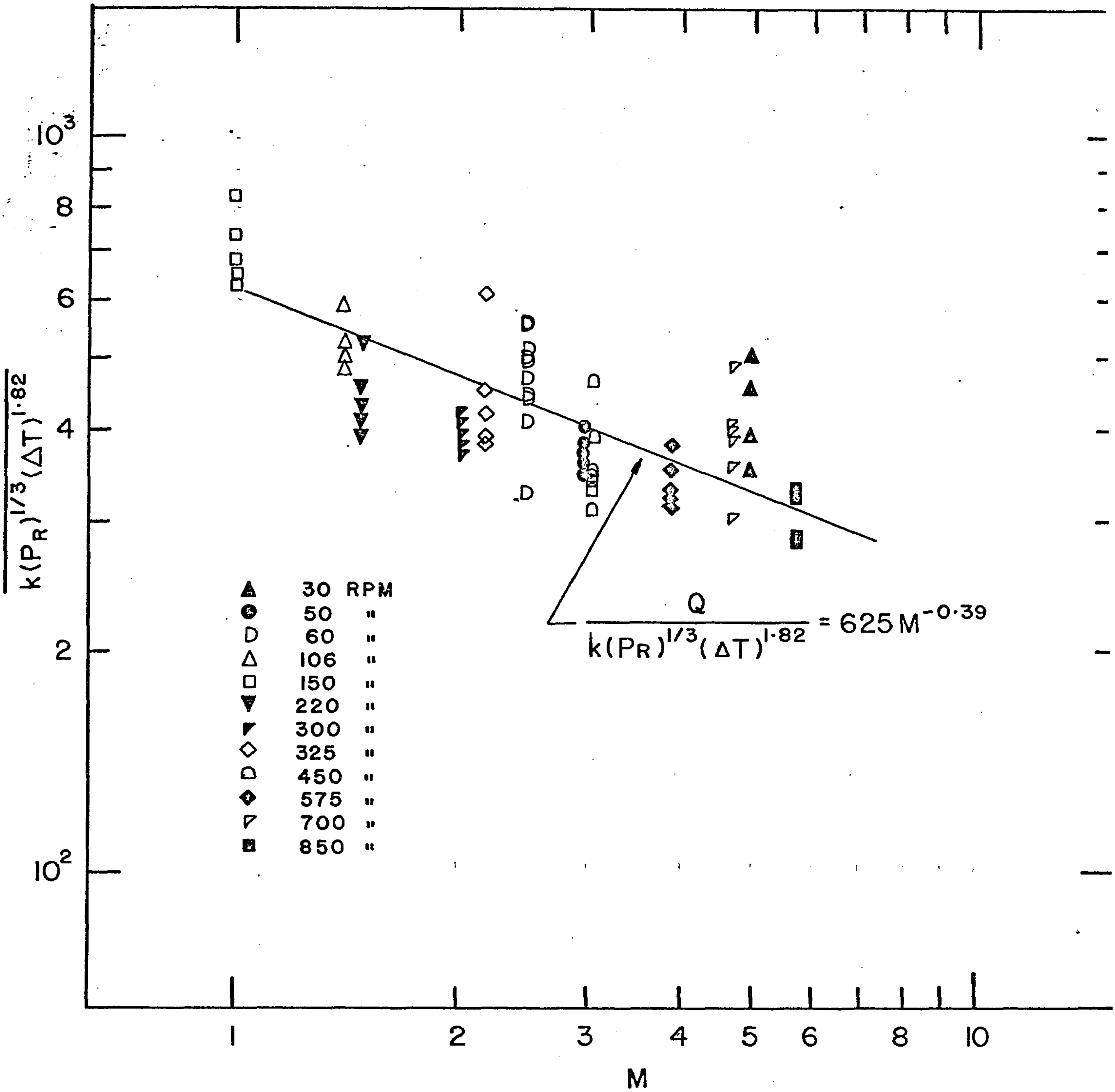

FIG. 14

CORRELATION ONE - EQUATION 5.4

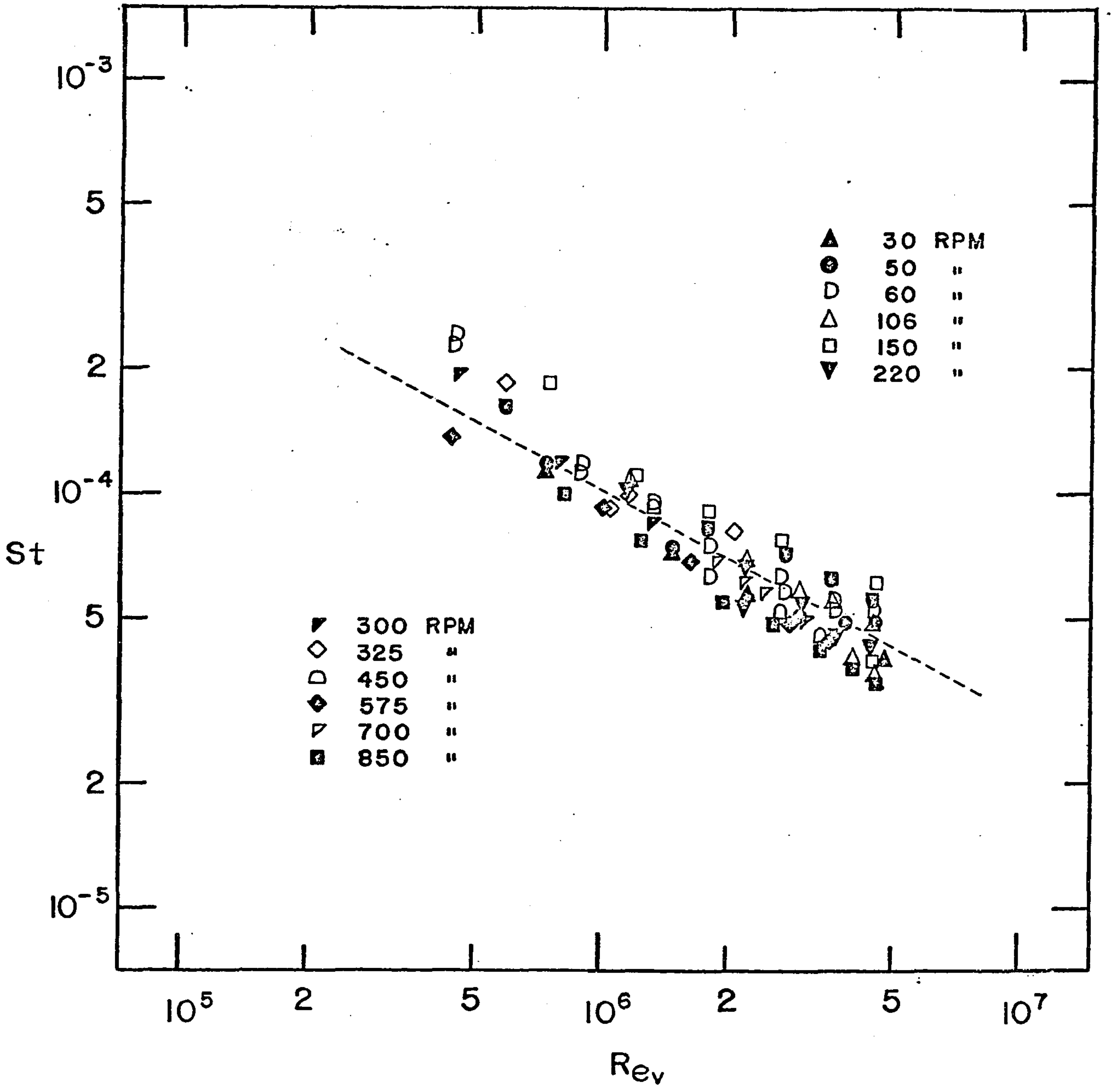

FIG. 15

RELATIONSHIP OF STANTON NUMBERS
AND VAPOUR REYNOLDS NUMBERS
FOR VARIOUS ROTATING REYNOLDS NUMBERS

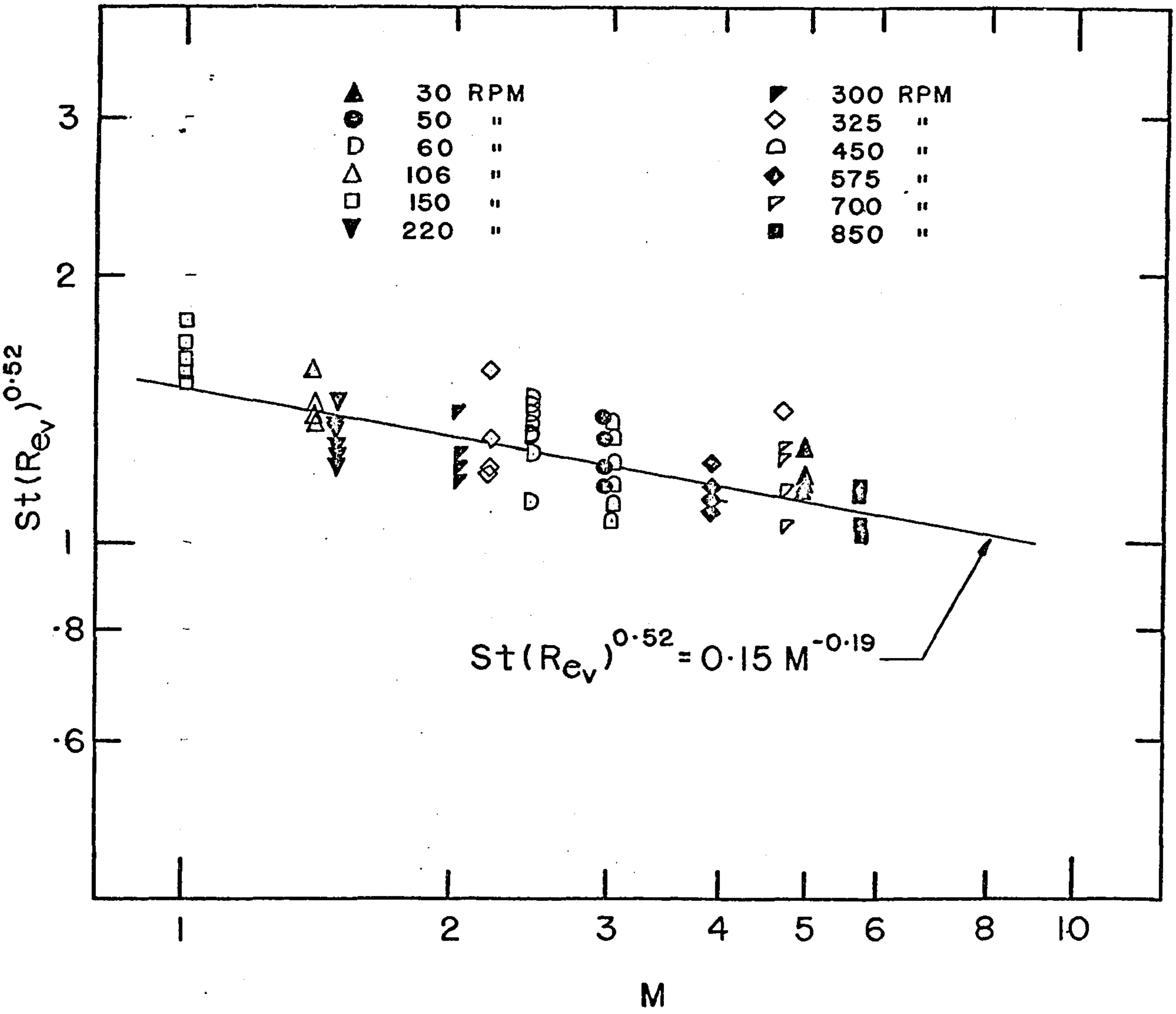

FIG. 16

CORRELATION TWO - EQUATION 5.7

APPENDIX I

PHOTOGRAPHS

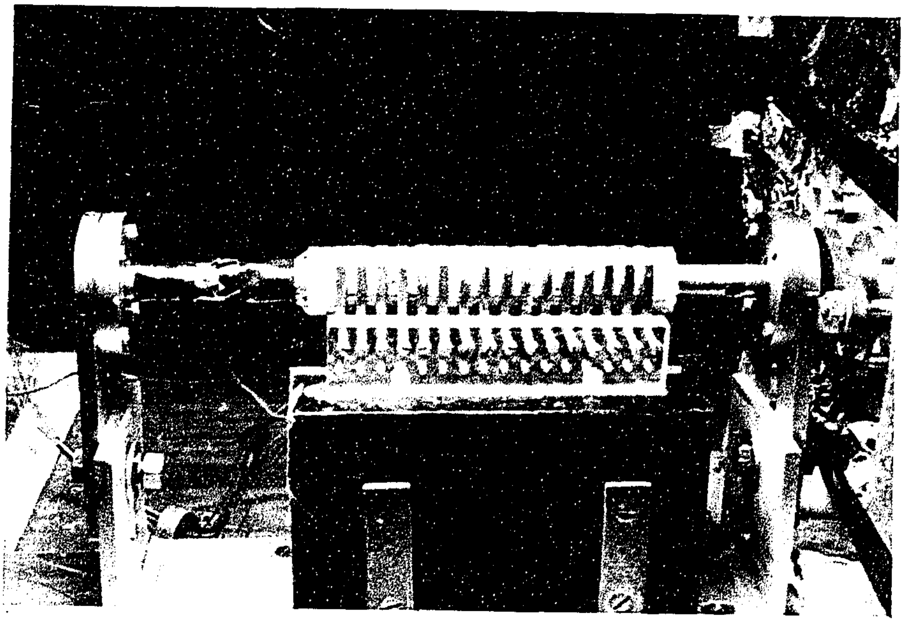

THERMOCOUPLE SLIP-RING ASSEMBLY

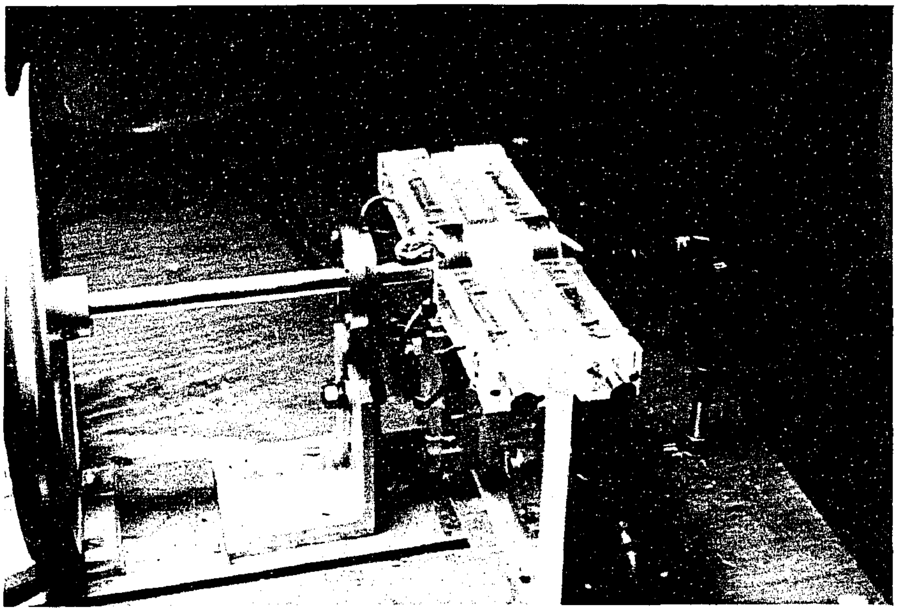

POWER SLIP-RING ASSEMBLY

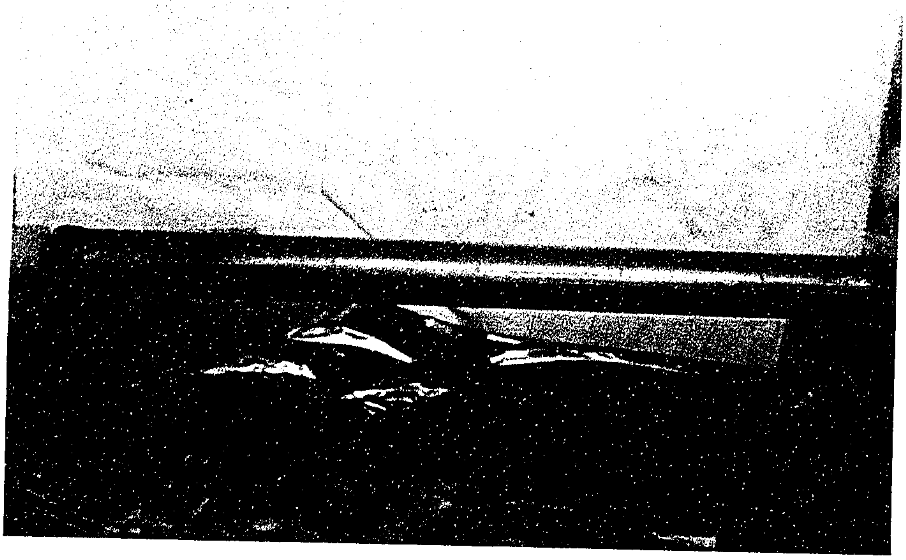

TEST SECTION

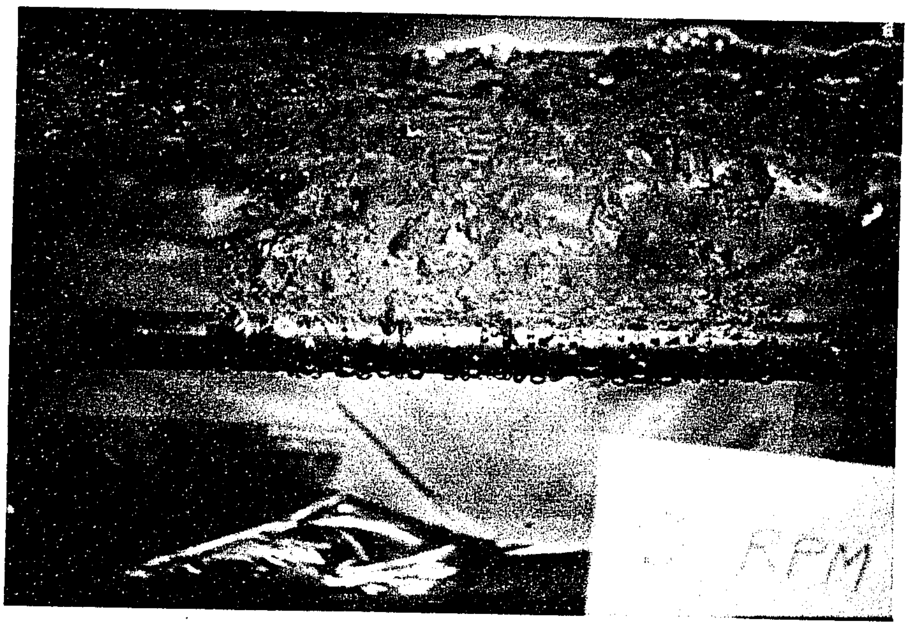

HEAT FLUX = 16,000 Btu/hr-ft^2

SPEED = 0 RPM

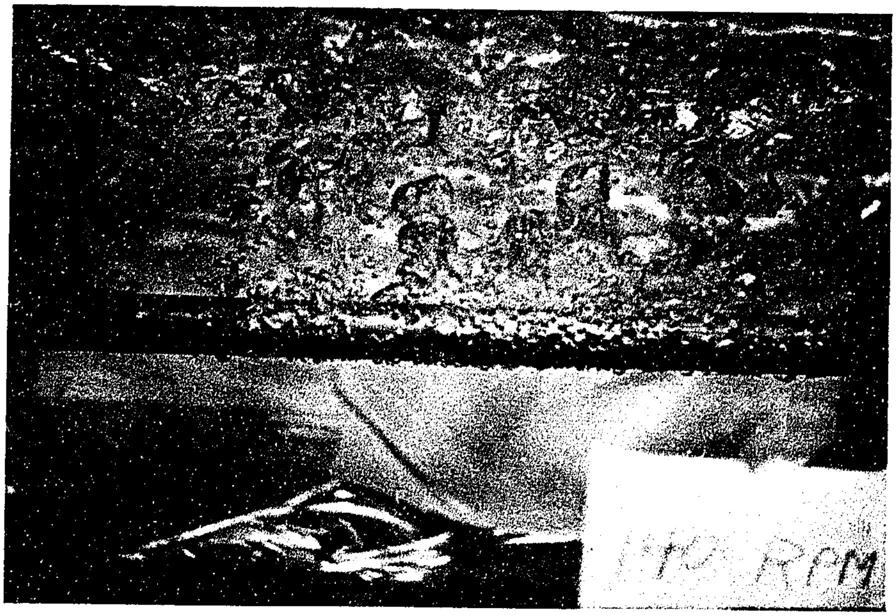

HEAT FLUX = 16,000 Btu/hr-ft^2

SPEED = 140 RPM

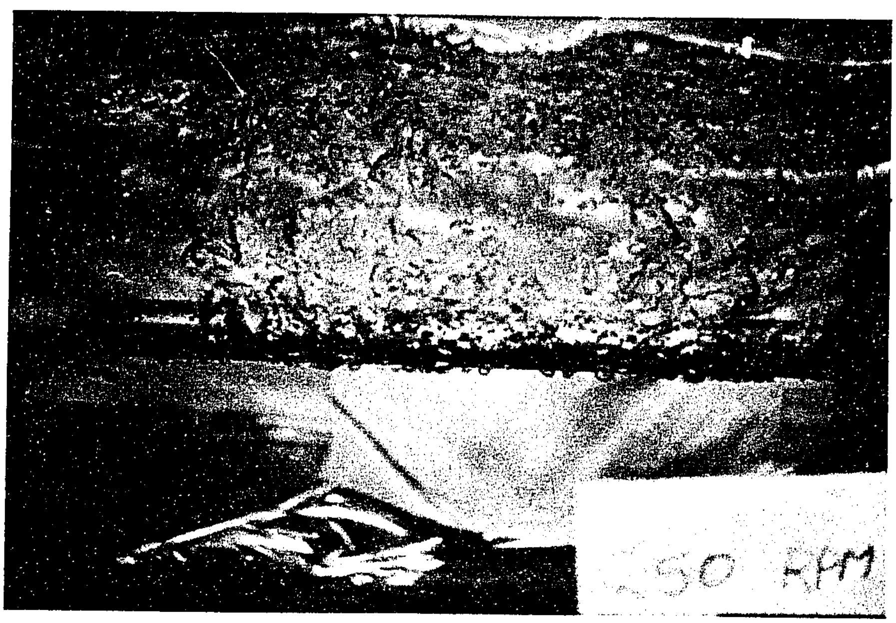

HEAT FLUX = 16,000 Btu/hr-ft^2

SPEED = 250 RPM

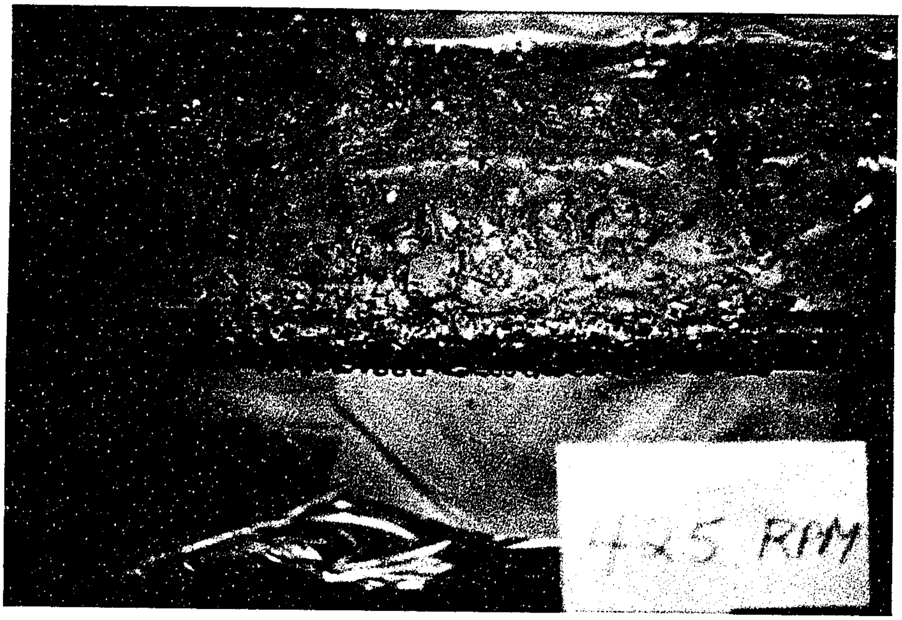

HEAT FLUX = 16,000 Btu/hr-ft^2

SPEED = 425 RPM

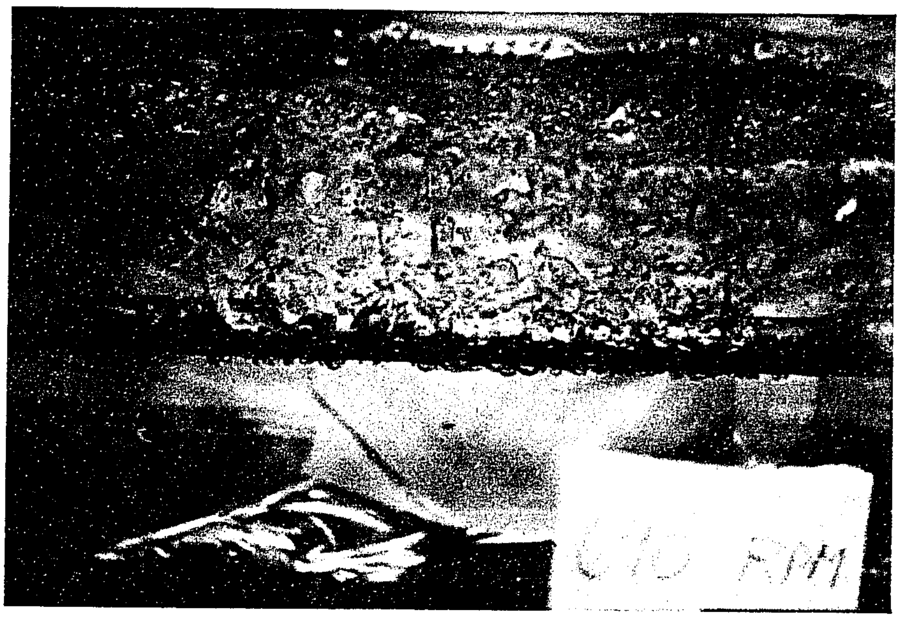

HEAT FLUX = 16,000 Btu/hr-ft^2

SPEED = 690 RPM

APPENDIX II

D A T A

RUN NO.	SPEED (RPM)	HEAT FLUX ($Btu/hr\text{-}ft^2$)	ΔT_{SAT} (°F)
1	30	8080	8.6
2	30	12120	10.6
3	30	16160	11.8
4	30	21010	12.6
5	30	24240	12.8
6	50	4040	5.4
7	50	8080	8.4
8	50	12120	10.8
9	50	16160	12.3
10	50	21010	14.1
11	50	25860	15.5
12	60	4850	5.2
13	60	9700	8.3
14	60	14540	9.7
15	60	19390	11.2
16	60	24240	12.2
17	60	4850	5.6
18	60	7270	6.5
19	60	9860	10.0
20	60	14710	10.9
21	60	19390	11.8
22	60	24240	12.1
23	106	6460	5.7
24	106	12120	9.0
25	106	16160	10.6
26	106	20200	11.4
27	106	23430	12.7
28	150	6460	5.5
29	150	9700	6.8
30	150	14540	7.9
31	150	19390	9.6
32	150	24240	9.7
33	220	6460	6.1
34	220	12120	9.2
35	220	16160	11.2
36	220	20200	13.4
37	220	24240	14.4
38	300	7270	7.5
39	300	12120	10.3
40	300	16160	11.4
41	300	20200	13.8
42	300	24240	14.8
43	325	5660	6.7
44	325	11310	7.6
45	325	16160	10.9
46	325	20200	13.4

RUN NO.	SPEED (RPM)	HEAT FLUX (Btu/hr-ft^2)	ΔT_{SAT} (°F)
47	325	24240	14.3
48	450	7270	6.9
49	450	9700	8.9
50	450	12120	10.7
51	450	14540	12.0
52	450	17780	13.7
53	450	21010	15.5
54	450	24240	15.7
55	575	5660	6.7
56	575	8890	9.0
57	575	12120	11.4
58	575	15350	12.5
59	575	18580	14.2
60	575	21820	15.7
61	575	25050	16.5
62	700	6460	6.3
63	700	10500	9.1
64	700	13740	10.6
65	700	16970	12.8
66	700	21010	14.4
67	700	24240	17.2
68	850	4360	6.3
69	850	6790	8.1
70	850	10500	11.3
71	850	13740	12.8
72	850	17780	15.0
73	850	21010	16.2
74	850	24240	17.6

VITA AUCTORIS

1942 Born in Leamington, Ontario, Canada on November 15.

1961 Graduated from Leamington District High School, Leamington, Ontario (senior matriculation).

1965 Received the degree of Bachelor of Applied Science in Mechanical Engineering from the University of Windsor, Windsor, Ontario.

1965 Awarded the Board of Governors Gold Medal for Proficiency in Mechanical Engineering.

1965 Awarded the Association of Professional Engineers of Ontario Gold Medal for Academic Achievement.

1966 Currently serving in the RCAF (aircrew) as an Electronics Systems Officer and a candidate for the degree of Master of Applied Science in Mechanical Engineering at the University of Windsor, Windsor, Ontario.